



NTNU – Trondheim
Norwegian University of
Science and Technology

Frequency-domain Method for
Global Dynamic Response Analysis of
a Semi-submersible Floating Wind Turbine

Guodong Liang

MASTER'S THESIS

Department of Marine Technology

Norwegian University of Science and Technology

June 2018

Trondheim, Norway

Supervisor: Zhen Gao, Professor, NTNU

Co-supervisor: Karl Merz, Doctor, SINTEF Energy Research AS

Jonas Ringsberg, Professor, CTH

Preface

This is a report of a Master thesis project carried out during the spring semester in the academic year 2017-2018. This project is a part of the study program - Nordic Master in Maritime Engineering, which is a dual-degree cooperation program between Marine Technology department at NTNU and Mechanics and Maritime Sciences department at CTH. This project is also a collaborative research with SINTEF Energy Research AS. The report includes a brief literature review on applications of frequency-domain methods developed for offshore wind turbines, methods applied and procedures performed to establish a linear dynamic model for the modified WindFloat concept design, and comparisons between the developed linear dynamic model and time-domain methods.

The project has been challenging and fairly interesting to work on. The debugging work to find out the errors was a bit stressful at the end. However, the feeling could not be better when the problems were eventually fixed. Due to some technical issues, the full wind turbine model was delivered in a quite late stage. Therefore the research mainly focuses on the below-rated loading condition.

The readers should preferably have some basic knowledge of hydrodynamics and dynamic analysis of offshore wind turbines.

16th June 2018, Trondheim, Norway

梁国栋

Guodong Liang

Acknowledgment

This report is written as the final result of a Master thesis project executed at marine technology department, NTNU. The topic is chosen based on the author's interest and skills. The project originated from my supervisor Professor Zhen Gao's suggestions.

I would like to express my deep gratitude to Professor Zhen Gao for his patient guidance and constructive suggestions during the planning and development of this Master thesis project. His willingness to provide help so generously has been very much appreciated.

I would also like to express great appreciation to Karl Merz, my co-supervisor, for providing the linearized wind turbine model and invaluable assistance. A great thanks to Professor Jonas Ringsberg for being my co-supervisor at CTH and providing useful suggestions.

Special thanks should be given to Professor Erin Bachynski for providing the modified Wind-Float model and professional support. My grateful thanks are extended to Kristine Bøyum Riste for the WADAM analysis result and to Yuna Zhao, Shi Deng, Zhiyu Jiang and Chengyu Luan for useful help and valuable discussions.

Finally, I wish to thank my family for their support and encouragement throughout my study.

16th Jun. 2018, Trondheim

Guodong Liang

Summary

The wind energy market is increasing. Developing offshore wind turbines has several advantages. Conventional time-domain methods in global dynamic response analysis are time-consuming. Inspired by this, the frequency-domain method in global dynamic response analysis has been studied in this Master thesis project for a semi-submersible floating wind turbine, modified WindFloat concept.

A linear dynamic model in frequency-domain has been established for the floating wind turbine, under a certain environmental condition. The model is developed by defining the constraint relationship between a linearized wind turbine model and a simplified model of the semi-submersible floater. To validate the linear dynamic model, fully coupled time-domain simulations have been run for the same design in a simulation tool - SIMA workbench. Turbulent wind fields generated from a turbulent-wind simulator TurbSim have been used as environmental inputs in the time-domain simulations, while rotor-average wind speed spectrum has been computed and applied in the linear dynamic model.

Spectrum analyses have been performed on the results obtained from different methods by considering wave-only, wind-only and combined wind and wave conditions respectively. The comparison results indicate that the developed linear dynamic model is able to give reasonable estimates in general, though an underestimation is observed when aerodynamic loads have been taken into account, which might be due to the linearization and simplification performed.

Contents

- Acknowledgment ii
- Summary v
- Contents vi
- List of Figures viii
- List of Tables x
- Nomenclature xii

- 1 Introduction 1**
- 1.1 Background 1
- 1.2 Objective 7
- 1.3 Report outline 7

- 2 Literature Review 9**
- 2.1 Time-domain and frequency-domain analysis 9
- 2.2 Frequency domain analysis for floating wind turbine 12
- 2.3 Environmental condition 14
- 2.4 Basic aerodynamic theory 15
- 2.5 A linear state-space offshore wind turbine model 16

- 3 Methodology 19**
- 3.1 Floater response analysis 19
- 3.2 Wind turbine response analysis 22
- 3.3 Floater and wind turbine coupling 26
- 3.4 Solve equation of motion in frequency domain 33
- 3.5 Spectrum analysis 33
- 3.6 Eigenvalue problem 36

4	Modelling and Procedures	39
4.1	Modified WindFloat concept	39
4.2	Loading conditions	42
4.3	Turbulent wind field	43
4.4	Time-domain simulation	47
4.4.1	SIMA model	47
4.4.2	Simulation and post-processing	48
4.5	Linear dynamic model	49
4.5.1	Environmental input	49
4.5.2	Floater model	50
4.5.3	Wind turbine model	53
4.5.4	Constraint equations	53
4.5.5	Post-processing	54
5	Results and comparison	57
5.1	Natural period comparison	57
5.2	Platform motion transfer function comparison	58
5.3	Spectrum analysis	60
5.3.1	Combined wind and wave condition	60
5.3.2	Wave only condition	66
5.3.3	Wind only condition	68
5.3.4	Discussion	73
6	Summary and Further Work	75
6.1	Summary	75
6.2	Further work	76
	Bibliography	77
A	Parameter settings in TurbSim input file	81
B	Time vector for different variables in SIMA results	83
C	Jonswap wave spectrum	85
D	Description of the content in the attached zip-file	87

List of Figures

- 1.1 Share of new renewable power installations in the EU, Total: 23,935 MW (2017) [38] 2
- 1.2 Cumulative and annual offshore wind energy installation in the EU [26] 3
- 1.3 Share of substructure types for grid-connected wind turbines (units) [26] 4
- 1.4 Typical floating wind turbine foundation designs [11] 5

- 3.1 Linear dynamic model 20
- 3.2 Coordinate systems used in the structural model [33] 23
- 3.3 Procedures for calculating aerodynamic loads 24

- 4.1 The WindFloat design (without mooring system) [40] 40
- 4.2 Turbulent wind field in TurbSim [17] 44
- 4.3 Power Law wind speed profile 46
- 4.4 SIMA model used in time domain simulations 47
- 4.5 Jonswap wave spetrum 49
- 4.6 Rotor-average wind speed spectrum 50
- 4.7 The developed linear dynamic model 54

- 5.1 Transfer function from wave elevation to platform motion-surge 58
- 5.2 Transfer function from wave elevation to platform motion-heave 59
- 5.3 Transfer function from wave elevation to platform motion-pitch 59
- 5.4 Transfer function from wind speed to platform motion-pitch 60
- 5.5 Wave spectra in combined condition 61
- 5.6 Wind speed spectra in combined condition 62
- 5.7 Wind speed spectra in combined condition (log scale) 62
- 5.8 Wave force spectra in combined condition 63

5.9 Pitch motion response spectra in combined condition	64
5.10 Pitch motion response spectra in combined condition (log scale)	64
5.11 Tower base bending moment spectra in combined condition	65
5.12 Tower base bending moment spectra in combined condition (log scale)	66
5.13 Wave spectra in wave only condition	67
5.14 Wave force spectra in wave only condition	67
5.15 Pitch motion response spectra in wave only condition	68
5.16 Wind speed spectra in wind only condition	69
5.17 Wind speed spectra in wind only condition (log scale)	69
5.18 Pitch motion response spectra in wind only condition	70
5.19 Pitch motion response spectra in wind only condition (log scale)	71
5.20 Tower base bending moment spectra in wind only condition	71
5.21 Tower base bending moment spectra in wind only condition (log scale)	72

List of Tables

- 2.1 Environmental statistics of Site 14 [25] 14

- 4.1 Design parameters of the NREL 5-MW wind turbine [19] 40
- 4.2 Operation parameters of the NREL 5-MW wind turbine [19] 41
- 4.3 Important parameters of the semi-submersible floater [20] 41
- 4.4 Natural periods of the modified WindFloat design concept [20] 42
- 4.5 Loading conditions determined for analyses [29] 43

- 5.1 Natural periods comparison 57
- 5.2 Peak value in transfer function from wind speed to platform motion 60
- 5.3 Comparison: wave spectra-combined condition 61
- 5.4 Comparison: wind speed spectra-combined condition 62
- 5.5 Comparison: pitch motion response-combined condition 64
- 5.6 Comparison: tower base bending moment-combined condition 65
- 5.7 Comparison: wave spectra-wave only condition 66
- 5.8 Comparison: pitch motion response spectra-wave only condition 68
- 5.9 Comparison: wind speed spectra-wind only condition 70
- 5.10 Comparison: pitch motion response spectra-wind only condition 70
- 5.11 Comparison: tower base bending moment spectra-wind only condition 72

- A.1 Parameter settings in TurbSim input file 81

- B.1 Time vectors for variables in SIMA results 83

Nomenclature

Abbreviation

DOF	Degree of freedom
TLP	Tension leg platform
SSWT	Semi-submersible wind turbine
SRA	SIMO-RIFLEX-AeroDyn
BEM	Blade element momentum method
FFT	Fast Fourier transform
PSD	Power spectrum density
SWL	Sea water line
STD	Standard deviation
SIMA	Simulation Workbench for Marine Applications
VAWT	Vertical axial wind turbine
HAWT	Horizontal axial wind turbine
FAST	Fatigue, Aerodynamics, Structures and Turbulence Code
WAMIT	Wave Analysis at MIT

Chapter 1

Introduction

This is the report of a Master thesis research project. The main purpose of this research project is to establish a complete frequency-domain model for a semi-submersible floating wind turbine - modified WindFloat concept design. In this chapter, the motivation of this research will be stated in section 1.1 with a general introduction of the background. The objectives of this Master thesis project will be listed in section 1.2 and an overview about the report structure will be given in section 1.3.

1.1 Background

Due to the limited deposit and pollution issues of conventional fossil energy, renewable energy starts to have a significant growth in the energy market as an inevitable trend of technology development. From the statistics published by U.S. Energy Information Administration [10], in the US, the electricity power generated from renewable sources (excluding hydroelectric and solar) in 2016 is approximately three times larger than the amount in 2007. Besides solar and hydroelectric energy, wind energy is also a considerable resource for power generation from renewable energy and its development is fast. From the statistics published by WindEurope [38] in 2017, wind energy devices take 65.3 % of the new renewable energy installations in the EU, as shown in figure 1.1. In Denmark, 43 % of the power generated comes from wind energy in 2017 [39].

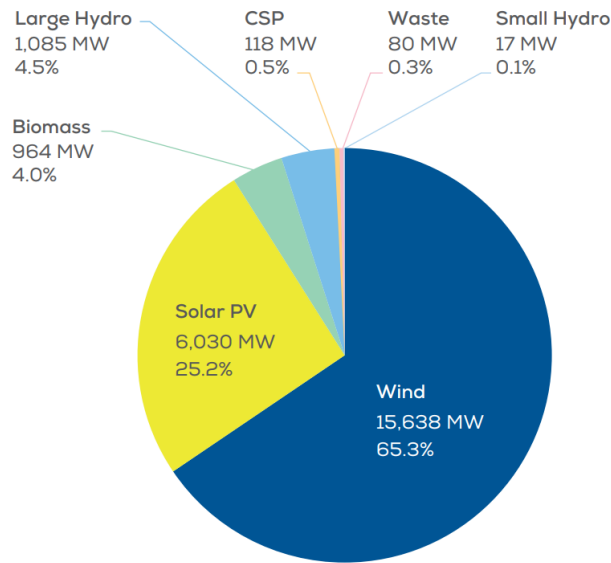
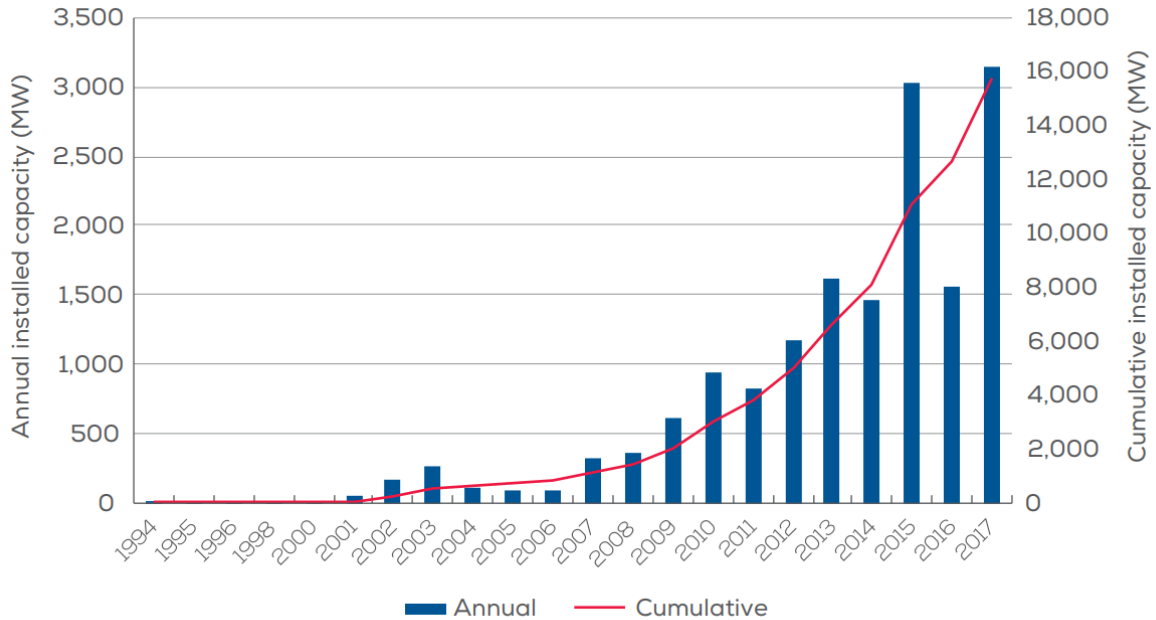


Figure 1.1: Share of new renewable power installations in the EU, Total: 23,935 MW (2017) [38]

Wind turbine is the most commonly used device of wind energy utilisation. It transforms the kinetic energy in the wind to the mechanical energy of the rotor through blade rotation. Then the mechanical energy is further transformed into electrical energy by a generator in the nacelle. Depending on the direction of the shaft axis, wind turbines are divided into two categories, vertical axial wind turbine (VAWT) and horizontal axial wind turbine (HAWT). Alternatively, it can be categorized as land based wind turbine or offshore wind turbine based on environment of the installation site.

As a conventional and mature power generation device, land based wind turbine has been applied and developed for several decades while the offshore wind farm is still an emerging concept. Offshore wind turbine has several advantages compared with land based wind turbine. In offshore areas, there is more available space with lower price. The avoidance from noise and visual impacts is also a big advantage. Furthermore, offshore wind load is stronger and more stable. As in equation 1.1, the available power in the wind is proportional to the cube of wind velocity, which means with a higher wind speed, there is more abundant wind energy that can be utilised in offshore region. These advantages make it worth developing offshore wind power generation devices. An observable increase in the total power of offshore wind energy installations in the EU can be caught from figure 1.2.

$$P_w = \frac{\rho_A A u^3}{2} \quad (1.1)$$



Source: WindEurope

Figure 1.2: Cumulative and annual offshore wind energy installation in the EU [26]

A variety of different theories have been applied to maintain the offshore wind turbine stability in order to have a stable and continuous power output. Both bottom-fixed and floating offshore wind turbines have been developed. Bottom-fixed wind turbines are the majority of the installed offshore wind turbine, as shown in figure 1.3. Main types of foundation for bottom-fixed wind turbine are monopile, gravity base, jacket, tripod and tripile.

However, due to natural technological limitations, bottom-fixed wind turbine has limitation in operating water depth. Floating wind turbine becomes more practical and competitive when the water depth in the offshore site exceeds 50m. For countries with less shallow water coastal region, like Norway and USA, floating wind turbines provide an approach to make use of the inexhaustible wind energy in the ocean. The first floating wind farm, Hywind Scotland, has started production since October, 2017 [41]. The wind turbines in Hywind Scotland wind farm are designed with spar foundations.

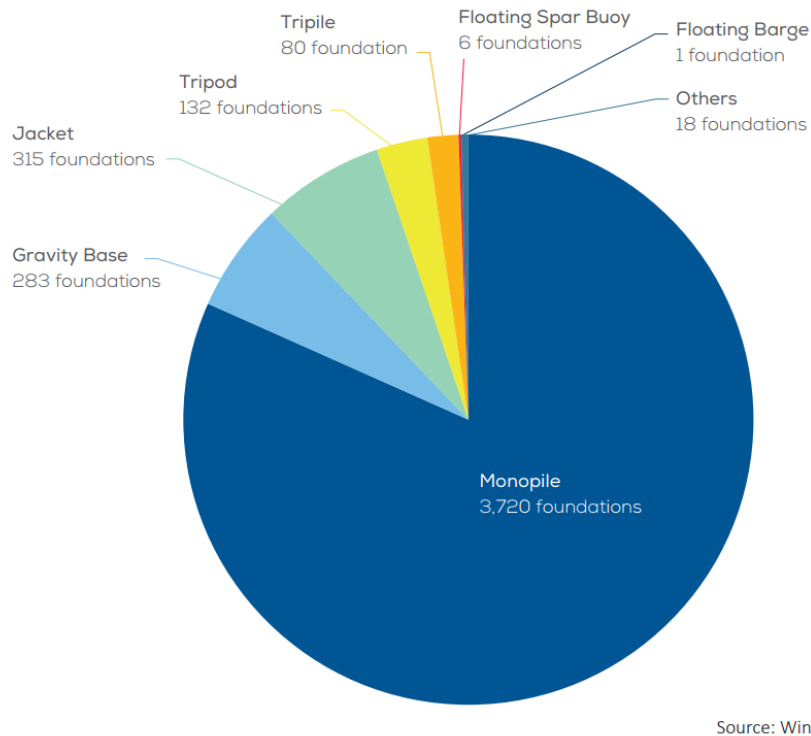


Figure 1.3: Share of substructure types for grid-connected wind turbines (units) [26]

A lot of foundation designs have been developed for floating wind turbine, among which, Spar, Tension leg Platform (TLP) and semi-submersible are the most common ones currently [9]. These three different foundation designs are illustrated in figure 1.4. They are developed based on different stability criteria. Spar is ballast stabilized. Semi-submersible is buoyancy stabilized and TLP is mooring line stabilized. Compared with each other, all of them have pros and cons with respect to motion characteristics, installation costs and operating water depth. For spar foundation, it has relatively small motion due to small water plane area, especially in heave direction. However, it requires a large operating water depth to maintain stability. Though semi-submersible wind turbine (SSWT) is more flexible with respect to water depth, it undertakes large wave loads because of its large water plane area. For TLP foundation, it has small footprint area on seabed compared with others and also small motion in heave, roll and pitch direction due to the restoring stiffness from tension legs. It is also flexible to operating water depth. But the installation for TLP wind turbine is challenging and costly.

In 2011, a full scale floating wind turbine, WindFloat, was developed and tested by Principle Power in a site 5Km off the coast of Portugal [40]. It is a semi-submersible floater assembled

together with a 2 MW Vestas wind turbine. The modified WindFloat foundation, which will be studied in this project, is developed based on this full scale floating wind turbine.

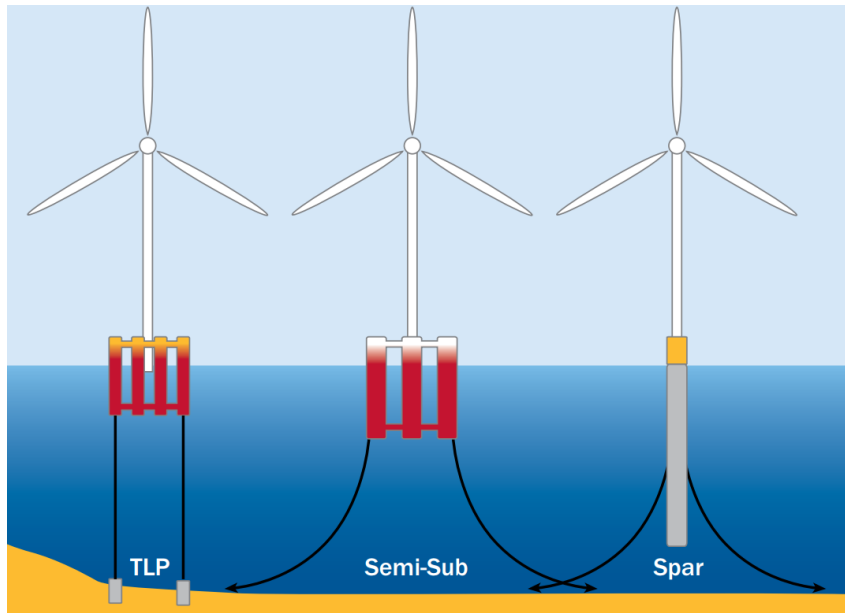


Figure 1.4: Typical floating wind turbine foundation designs [11]

Benefiting from extensive space available in the ocean and also considering economies of scale to cover the cost, wind turbines with higher capacity and larger scale have been designed and studied. Two typical large scale wind turbines are a 5MW reference wind turbine designed by the National Renewable Energy Laboratory (NREL) in 2009 [19] and a 10MW reference wind turbine designed by Technical University of Denmark (DTU) in 2013 [6]. The NREL 5 MW wind turbine will be assembled together with the floater in this project.

As there are advantages mentioned above to develop floating wind turbines, global dynamic analysis becomes critical because of the hostile ocean environment and ever-changing loading conditions. When performing global analysis of large floating offshore structures, usually the environment inputs are two parameters coming from wave loads: significant wave height and wave period. But for floating wind turbines, mean wind speed should also be considered as an environment input.

When it comes to global dynamic analysis of floating wind turbine, time-domain methods are usually preferred due to the strong coupling effects found between wind- and wave-induced loads and responses. Various time-domain methods have been developed for this purpose, such as FAST (Fatigue, Aerodynamics, Structures and Turbulence) Code [18] and

SIMO-RIFLEX-AeroDyn (SRA) tool [21]. The FAST code was initially made for land-based wind turbine and it was extended for offshore wind turbine by including hydrodynamic loads [18]. SIMO-RIFLEX-AeroDyn model was developed by combining SIMO-RIFLEX (hydrodynamic, structural, and control system computational tools from MARINTEK) and AeroDyn model which accounts for aerodynamic loads [21]. In this project, the results from developed frequency-domain model will be compared with time-domain simulation results in SIMA workbench (MARINTEK), which is based on the SRA tool .

Time-domain analysis is usually time-consuming and requires significant computational effort. Especially in some design codes, e.g. IEC 61400-3 [15], a large amount of load cases are required to be checked during the design process of offshore wind turbine. As an alternative, it is noticed that frequency-domain methods have been developed for fatigue analysis of offshore oil and gas platform, in which linear and second order wave loads and response are considered. For example, a frequency-domain procedure is suggested for the response analysis of column-stabilized units in DNV Recommended Practice (DNV-RP) [8]. The non-linearity in wave-induced response mainly comes from viscous forces, catenary mooring lines and large platform displacements. Similarly, it is considered that if the dominant environmental conditions are moderate and the induced non-linear effects are not significant, frequency-domain methods with linearized model may be sufficient in the wave-induced response analysis for floating wind turbine, especially in the preliminary design stage.

However, the aerodynamic loads acting on the wind turbine rotor are significant and typically non-linear, which makes linearization of the non-linear aerodynamic loads essential before frequency-domain methods could be applied. In a Sintef Energy research report [34], Karl Merz has developed a frequency-domain method for dynamic response analysis of a monopile-foundation offshore wind turbine. In that report, a method is introduced for linearizing the aerodynamic loads acting on the wind turbine. It is also mentioned in the report that with proper consideration, the method could also be applicable for other type of wind turbine foundations. A frequency-domain method for hydrodynamic response analysis of the modified WindFloat concept has been studied in a previous Master thesis [29].

Based on these previous researches, this project is set to develop a simplified linear dynamic model for the global dynamic response analysis of the semi-submersible floating wind turbine-modified WindFloat.

1.2 Objective

The main objective of this Master thesis project is to develop a simplified linear dynamic model for global dynamic response analysis of a semi-submersible floating wind turbine in frequency domain. This can be achieved by performing following procedures:

1. Literature review on both time-domain and frequency-domain analysis methods for coupled dynamic analysis of offshore wind turbines due to wind and wave loads.
2. Establish a complete frequency-domain model for the semi-submersible floating wind turbine considering both aerodynamic and hydrodynamic loads.
3. Perform dynamic response analyses using the developed frequency-domain model for selected wind and wave conditions and obtain the spectra of interested response parameters.
4. Compare the results from the frequency-domain model with those from the direct time-domain simulations.

1.3 Report outline

This Master thesis report is structured as follows:

- In Chapter 1, the background of this Master thesis project is introduced and the objectives to be achieved are listed.
- In Chapter 2, a literature review, which has been performed on relevant topics and reseaches, is presented.
- In Chapter 3, the methods which have been applied to develop the linear dynamic model are explained.
- In Chapter 4, the modified WindFloat concept design is introduced. The modelling work and procedures performed are also presented.
- In Chapter 5, the results and comparisons are presented, together with discussions on the results.

- In Chapter 6, a summary of this Master thesis project is made and suggestions for improvement and further development are listed.

Chapter 2

Literature Review

In this chapter, a literature review, which has been performed on relevant topics and researches, will be briefly presented. A summary of relevant time-domain and frequency-domain researches will be discussed in section 2.1. Basic procedures of a simplified frequency domain analysis for a floating wind turbine will be given based on the research by Kvittem and Moan [22] in the following section. In section 2.3, a research on the environmental conditions will be presented [25], based on which the loading conditions for this project have been decided. Some basic aerodynamic theory will be introduced in section 2.4. In the last section, a linear state-space offshore wind turbine model developed by Karl Merz [34] will be introduced.

2.1 Time-domain and frequency-domain analysis

Since offshore floating structures suffer periodic wave loads through their full service lives, fatigue damage is a critical issue. To perform fatigue analysis, the detailed information of loads acting on critical structural components is required. For conventional floating structures like oil platform, fatigue assessment can be performed in frequency-domain because of the effective linearization for wave loads. However, when applying frequency-domain methods for floating wind turbines, extra attention should be given due to the non-linear aerodynamic loads and strong coupling effects between wind and waves.

To perform time-domain analysis, the time series of relevant loads or stresses are usually

required as inputs. A problem with floating wind turbine is that there is a lack of full-scale testing data. According to Bachynski et al [3], it is actually difficult to get accurate results from wind turbine model tests, since wind and waves are scaled to model scale by different constants. Wind is scaled by Reynolds number while waves are scaled by Froude number. Therefore a different method applied in model test has been developed by Bachynski et al [3]. The wind loads acting on the turbine were represented by forces applied on top of the tower through a frame. The forces need to be applied were calculated by advanced programming and based on real-time loading and responses. While the hydrodynamic loads were still excited by waves. The author has visited one of the model tests in the ocean basin at Marinteknisk centre. In addition to time series obtained from real test, as mentioned in section 1.1, several simulation tools have been developed to perform software simulations in time-domain.

A time-domain fatigue analysis of a semi-submersible wind turbine has been performed by Kvittem and Moan [23]. This research is aiming at finding the necessary simulation duration which could capture critical effects from slowly varying loads and the maximum bin size for the discretization of the joint wind and wave distribution. Totally 2216 fully coupled time-domain simulations have been run in SIMO-RIFLEX-AeroDyn tool. The results show that important fatigue effects can be obtained by 1 hour simulation while 3-6 hours simulation is needed to capture the slow varying responses because of the large natural periods of the wind turbine structure studied. The misalignment between wind and waves has also been considered in this research. The results show that unidirectional wind and wave condition gives the most critical fatigue damage, while the wave direction mainly determines which part of the floater experiences the highest fatigue damage. This has also been observed in another research by Bachynski et al [4] on the effect of misaligned wind and waves for several different design concepts.

A research for a bottom-fixed offshore wind turbine has been done by Tempel [36], in which fatigue analysis and the uncoupling of wind turbine and support structure have been studied. The wind turbine was modelled on a rigid support and the transfer functions from turbulent wind speed to wind load acting on the tower top were generated. Then the transfer functions from the tower top load to bending stress and the transfer functions from wave height to bending stress were computed. The total stress response spectrum was obtained by computing the response spectra due to wind loading and wave loading separately and

then applying linear superposition. The results show that the stress spectra obtained from frequency-domain method match well with the stress spectra computed by time-domain method. The fatigue analysis performed by Tempel [36] is for a bottom-fixed offshore wind turbine and it shows good agreements between time-domain and frequency-domain methods.

A coupled analysis in frequency-domain was performed by Wayman et al for an offshore floating wind turbines with mooring system and operating water depth 10-200m [37]. To perform the coupled analysis, the FAST code was coupled with a wave load and response simulation code WAMIT (Wave Analysis at MIT). The coupled analysis was performed for two wind turbines with different floaters (one with shallow drafted barge and another with TLP). But the results have not been verified by time-domain simulation results or full-scale testing data.

A simplified linear frequency-domain analysis has been performed by Bachynski et al for a wind turbine concept with a four tension leg platform (TLP) [5]. The results have been compared with fully-coupled nonlinear time-domain simulations. It shows that for wave-only condition, the frequency-domain method can capture the trends of observed parameters, such as platform motions and dynamic tension. However the results are not accurate enough to be used for comparing the performance of different designs, especially for combined wind and wave conditions. Further improvements have been suggested.

Another comparison between time-domain and frequency-domain methods has been made by Kvittem and Moan [22], for fatigue analysis on the tower of a semi-submersible wind turbine. The bending moments and fatigue damage computed by frequency-domain methods have been compared with fully coupled, non-linear time-domain analyses. At the beginning, a rigid model has been used in the research, which gives an underestimation of the tower bending moments. By applying a generalized degree-of-freedom (DOF) model to include the flexibility of the tower and blades, the results have been improved. It also shows that the wind-induced bending moments in low frequency range were not captured well, which was due to the linearization according to the conclusion.

From previous researches, it can be seen that to do dynamic analysis in frequency domain, the terms in the equation of motion need to be linearized, which gives rise to the loss of excitation caused by nonlinear terms in some degree. In order to verify the frequency-domain

results, comparison with testing data or fully-coupled nonlinear time-domain simulation results is necessary. By comparing the results, improvements in the frequency-domain method might be achieved by taking into account some of the missed excitations.

2.2 Frequency domain analysis for floating wind turbine

A simplified frequency-domain analysis method applied for a floating wind turbines are summarised below, based on the study by Kvittem and Moan [22]. The governing dynamic equation of motion, which is a linear equation for 6 degree-of-freedom (DOFs), is expressed as:

$$(\mathbf{M} + \mathbf{A}(\omega))\ddot{\mathbf{X}}(\omega) + \mathbf{B}(\omega)\dot{\mathbf{X}}(\omega) + \mathbf{C}\mathbf{X}(\omega) = \mathbf{F}(\omega) \quad (2.1)$$

The external forces $\mathbf{F}(\omega)$ and structural response $\mathbf{X}(\omega)$ in the equation can be expressed as a function of frequency by using transfer functions in complex form. The wave loads can be expressed as a function of wave elevation with a complex transfer function ($\mathbf{H}_{\zeta\mathbf{F}}(\omega)$) as:

$$\mathbf{F}_{\text{wave}}(\omega) = \mathbf{H}_{\zeta\mathbf{F}}(\omega)\mathbf{e}^{i\omega t} \quad (2.2)$$

By solving the governing equation 2.1, the relationship between structural response $\mathbf{X}(\omega)$ and the wave induced force $\mathbf{F}^{\text{wave}}(\omega)$ can be expressed as:

$$\mathbf{X}_{\text{wave}}(\omega) = \mathbf{H}_{\mathbf{F}\mathbf{X}}(\omega)\mathbf{F}_{\text{wave}}(\omega) \quad (2.3)$$

Where $\mathbf{H}_{\mathbf{F}\mathbf{X}}(\omega)$ is the complex transfer function.

Then the transfer function which describes the relation between structure response and wave elevation can be found by equation 2.4.

$$\mathbf{H}_{\zeta\mathbf{X}}(\omega) = \frac{\mathbf{H}_{\zeta\mathbf{F}}(\omega)}{-\omega^2(\mathbf{M} + \mathbf{A}(\omega)) + i\omega\mathbf{B}(\omega) + \mathbf{C}} \quad (2.4)$$

Similarly, the structural response due to wind force acting on the turbine rotor can be de-

scribed by assuming that the wind load can be linearized and expressed by a complex transfer function $\mathbf{H}_{\mathbf{UF}}(\hat{\omega})$, where \mathbf{U} is the turbulent hub wind speed.

$$\mathbf{F}_{\text{wind}}(\hat{\omega}) = \mathbf{H}_{\mathbf{UF}}(\hat{\omega})\mathbf{U}(\omega) \quad (2.5)$$

In the research by Kvittem and Moan [22], the wind load acting on the rotor was calculated by finding the variance spectra of rotor forces with only wind excitation and ignoring the influence of wave induced motions on rotor forces. The amplitudes of structural motions were taken as linearization points for both wave- and wind-induced motions. As shown in equation 2.1, the damping force was considered as linearly related to the velocity of the structure. However, thrust force acting on the rotor, which was used to calculate wind load, and the viscous drag force acting on slender structural members, can be described better by quadratic velocity terms [22].

In terms of fatigue damage analysis, to get the time series of the evaluated parameters, an approximate inverse Fourier transform with random phase can be performed. For example:

$$M(t) = \sum_{k=1}^N \sqrt{2S_M(\omega_k)\Delta\omega} \cos(\omega_k t + \theta_k) \quad (2.6)$$

Where S_M is the spectral density function of the bending moment and θ is the generated random phase angle.

A list of procedures in frequency-domain analysis was suggested by Kvittem and Moan [22] as shown below.

- Establish the dynamic equilibrium equation for the system.
- Linearize the non-linear terms in the dynamic equilibrium equation by applying different theories.
- Solve the equation and get the complex transfer functions for structural motion responses.
- Establish the transfer functions between structure responses and parameters need to be evaluated (e.g. bending moment at tower base) and generate the spectrum of required parameters.

- Apply inverse Fourier transform to create the time series.
- Perform fatigue analysis based on the generated time series data.

2.3 Environmental condition

Bottom fixed wind turbine has relatively small induced motions caused by external loads. Therefore, the structural stresses can be calculated as wind- and wave- induced separately. Simple superposition on stress contributions is still valid, which has been verified in the research by Tempel [36]. Unlike the bottom-fixed wind turbine, structural analyses become more complex for floating wind turbine in coupled wind and wave loading conditions. With coupled wind and waves, one more parameter, the wind speed, should be taken into account when describing the environmental condition. Therefore, the number of load cases need to be checked increases.

The joint distributions of environmental conditions at five European offshore sites have been investigated by Li et al, as basis for the development of combined wind and wave energy devices [25]. In this research, hourly mean wind and wave hindcast data from 2001 to 2010 is taken as the database for the five selected sites, in which three sites (site 1, site 3 and site 5) are facing the Atlantic Ocean and two sites (site 14 and site 15) are located in the North Sea. By fitting the analytical distribution models to the hindcast data, long-term joint distributions have been computed. The marginal wind and wave distributions have also been studied for each of these five sites. The distribution parameters are provided in the published papaer. Among these five offshore sites, the site 14, 'Norway 5', is selected as the operating environment for the modified WindFloat concept studied in this project. Site 14 is located in the North Sea, outside the coast of Norway. Some statistics of site 14 are presented in table 2.1.

Table 2.1: Environmental statistics of Site 14 [25]

Parameter	Value	Unit
Water depth	202	m
Distance to shore	30	km
Average wind power density at 80m	1094.84	W/m ²
Average wave power density	46.43	kW/m

The wind power density and wave power density in table 2.1 indicates the wind energy resource and hydrodynamic loads which can be expected in site 14. Compared with other 17 sites, site 14 has the second largest average wind power density and the fourth largest average wave power density. Marginal distribution of wind speed and conditional distributions from this research will be used to decide the loading conditions in the thesis project.

2.4 Basic aerodynamic theory

The basic wind turbine aerodynamic theory can be found in Hansen [14]. In order to have a better understanding of wind turbine behaviours, some aerodynamic theory will be briefly introduced in this section, based on the lecture notes in course TMR4505 Integrated Dynamic Analysis of Wind Turbines [1].

Blade element momentum theory

The basic blade element momentum (BEM) theory is based on foil theory which can be found in Hansen [14]. It is developed from momentum theory and blade element theory. In BEM method, aerodynamic forces acting on the turbine blades are computed locally at the blade section, by using empirical lift and drag coefficients. Then the computed aerodynamic loads are balanced with momentum change of the air flowing through the rotor disk. An outline of how to apply BEM method in an iteration procedure can be found in the RIFLEX theory manual [28].

The basic BEM theory need to be modified by some important corrections. Based on different applications, corrections need to be considered may differ. Some typical corrections are introduced in the following part.

Prandtl correction

With finite number of blades, the downstream wake of the rotor plane is different from the one assuming infinite number of blades. This is because at the blade tip, the air does not pass through the blade section separately. It tends to flow around from lower side to upper side, which follows the pressure gradient. This tip loss effect results in less aerodynamic force produced at the blade tip and should be modified by Prandtl correction.

Glauert correction

The axial induction factor is defined as:

$$a = \frac{v_0 - v_A}{v_0} \quad (2.7)$$

Where v_0 is the undisturbed wind speed and v_A is the wind speed before the air flow passes rotor disk.

The BEM theory is not valid when the induction factor is larger than 0.5. Thus, Glauert correction should be applied to correct the thrust coefficient for a large induction factor.

Dynamic wake

The dynamic wake effect refers to the time lag in the induced wind velocity caused by shedding and downstream convection of vorticity [1]. In practice, it takes some time for a large flow field to react to the change in incoming wind speed, blade pitch angle or rotor speed. Therefore, there is a time delay before the induction factor actually updates. The dynamic wake effect can be considered in BEM method by applying Stig Øye dynamic inflow model.

Dynamic stall

The lift and drag coefficients used in BEM method are described as lift or drag curves. They are usually plotted as functions of angle of attack. However, in practice, when the wind turbine experiences dynamic incoming wind, attachment and re-attachment of the flow may occur on the blades. This will lead to the oscillation of the angle of attack, which means the lift and drag coefficients will not exactly follow the static curves. Several methods have been developed to take the dynamic stall effect into account, among which the Stig Øye model is implemented in the SIMO-RIFLEX-AeroDyn tool [28].

2.5 A linear state-space offshore wind turbine model

A linear state-space model of an offshore wind turbine has been developed by Karl Merz as a part of the STAS Wind Power Plant Analysis Program [34]. The linear state-space wind turbine model is based on a set of MATLAB/Octave scripts, from which, state matrices describing the linearized aeroelastic dynamics of the wind turbine can be generated [34]. The original model is developed for a bottom-fixed OC3 monopile foundation. As stated in the

report, with proper modifications, it could also be applied to other types of foundations [34].

The wind turbine model is established based on the momentum balance by considering time-lag caused by dynamic inflow, circulation lag and dynamic stall. The blade element momentum (BEM) method has been applied to calculate the aerodynamic loads acting on the turbine blades. The wind turbine structure is built by finite element beams. When establishing the governing equations, multi-body formulation with modal reduction has been applied to the tower, nacelle, drive-shaft and three blades. A steady-state operating point to be used in linearization is defined as inputs. The results/outputs are given in state matrix format which describes the fluctuation about the defined operating point. It should be noticed that the linearization is performed based on the defined operating point. Therefore, the developed model is not expected to give reasonable estimates if the system state is far away from the defined operating point, for example, in extreme loading condition.

The aerodynamic properties of the original linear state-space wind turbine model are defined based on the DTU 10 MW reference wind turbine [6]. It has been verified against other programs. The results of aerodynamic loads have been compared with time domain FAST/Aerodyn simulations. The results match well even for wind speed departing significantly from the operating point [34]. The results of structural dynamic analysis have been verified by Finite element analysis program [34].

In this Master thesis project, a linearized wind turbine model, based on the NREL 5MW reference wind turbine, has been provided by Karl Merz. The wind turbine model is linearized by applying the method developed in STAS report. Then it is connected together with a hydrodynamic model of the semi-submersible floater, which becomes the linear dynamic model developed for modified WindFloat concept.

Chapter 3

Methodology

In this chapter, the theory and methods which have been applied in this Master thesis project will be presented. To develop the linear dynamic model, a hydrodynamic model of the floater has been assembled, which will be introduced in section 3.1. The linearized wind turbine model will be described in section 3.2. Then the method used to connect these two parts together will be presented in section 3.3. How to solve the coupled model in frequency domain will be shown in section 3.4. In section 3.5, basic theory used in spectrum analysis will be introduced. How the eigenvalue problem is solved to obtain the structural natural frequency will be presented in section 3.6.

3.1 Floater response analysis

The linear dynamic model is illustrated in figure 3.1. The semi-submersible floater is considered as a rigid body. The mooring system has been simplified as horizontal spring stiffness in surge, sway and yaw directions. The linearized wind turbine is built by finite element beams and connected to the floater. Node P in the figure is the platform reference node. Node n refers to the node on the platform where the wind turbine is connected. Node F at the end of the tower is the foundation reference node.

For the floater, the governing equation of motion in 6 DOFs can be described as:

$$(\mathbf{M} + \mathbf{A}(\omega))\ddot{\mathbf{x}}(t) + \mathbf{B}(\omega)\dot{\mathbf{x}}(t) + \mathbf{C}\mathbf{x}(t) = \mathbf{f}_w(t) \quad (3.1)$$

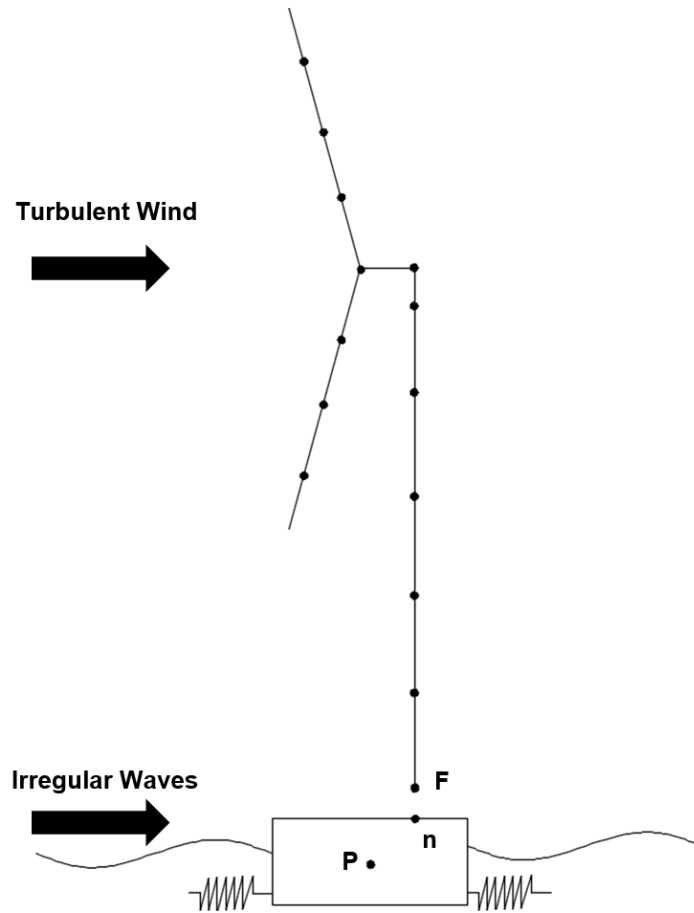


Figure 3.1: Linear dynamic model

where:

- \mathbf{M} is the mass matrix.
- $\mathbf{A}(\omega)$ is the frequency dependent added mass matrix.
- $\mathbf{B}(\omega)$ is the hydrodynamic damping matrix which includes both linear damping and frequency dependent damping.
- \mathbf{C} is the restoring matrix.
- \mathbf{f}_w is the hydrodynamic loads acting on the structure. In this project, only first order wave loads have been considered due to limited time.
- $\ddot{\mathbf{x}}, \dot{\mathbf{x}}, \mathbf{x}$ is the structure response.

In order to be assembled together with the wind turbine model, the governing equation of motion has been rewritten in a state-space format.

$$\begin{bmatrix} \mathbf{I} & \mathbf{0} \\ \mathbf{0} & \mathbf{M} + \mathbf{A}(\omega) \end{bmatrix} \frac{d}{dt} \begin{bmatrix} \mathbf{x} \\ \dot{\mathbf{x}} \end{bmatrix} = \begin{bmatrix} \mathbf{0} & \mathbf{I} \\ -\mathbf{C} & -\mathbf{B}(\omega) \end{bmatrix} \begin{bmatrix} \mathbf{x} \\ \dot{\mathbf{x}} \end{bmatrix} + \begin{bmatrix} \mathbf{0} \\ \mathbf{f}_w(t) \end{bmatrix} \quad (3.2)$$

Where \mathbf{I} is an identity matrix and $\mathbf{0}$ is a zero matrix.

Equation 3.2 is equivalent to equation 3.1. The first order wave loads can be describe as a function of wave elevation by a transfer function in complex format, as shown in equation 3.3.

$$\mathbf{f}_w(t) = \mathbf{H}_{\xi F}(\omega)\xi(t) \quad (3.3)$$

where:

- $\mathbf{H}_{\xi F}(\omega)$ is the first order wave force transfer function.
- $\xi(t)$ is the wave elevation.

Hence, equation 3.2 can be written as:

$$\mathbf{N}_P \frac{d}{dt} \mathbf{x}_P = \mathbf{A}_P \mathbf{x}_P + \mathbf{B}_P \xi(t) \quad (3.4)$$

Here the subscript P indicates 'platform', i.e. the floater. \mathbf{x}_P is the state vector of the floater.

$$\mathbf{x}_P = \begin{bmatrix} \mathbf{x} \\ \dot{\mathbf{x}} \end{bmatrix}$$

\mathbf{B}_P is defined as:

$$\mathbf{B}_P = \begin{bmatrix} \mathbf{0} \\ \mathbf{H}_{\xi F} \end{bmatrix}$$

Then the linear equation of motion of the floater can be expressed as:

$$\mathbf{N}_P \frac{d}{dt} \Delta \mathbf{x}_P = \mathbf{A}_P \Delta \mathbf{x}_P + \mathbf{B}_P \Delta \xi(t) \quad (3.5)$$

3.2 Wind turbine response analysis

Based on the STAS report [34], the method used to establish and linearize a wind turbine model will be briefly introduced below.

In general, the linear state-space wind turbine model can be described as:

$$\mathbf{N} \frac{d\mathbf{x}}{dt} = \mathbf{A}\mathbf{x} + \mathbf{B}\mathbf{u} \quad (3.6a)$$

$$\mathbf{y} = \mathbf{C}\mathbf{x} + \mathbf{D}\mathbf{u} \quad (3.6b)$$

Where:

- \mathbf{x} is a vector of system states
- \mathbf{u} is a vector of inputs
- \mathbf{y} is a vector of outputs (refer to any system variables which can be written as a linearized function of \mathbf{x} and \mathbf{u})
- \mathbf{N} is a modulus matrix.

Since multi-body formulation has been applied in this model [34], the governing equation for each module can be written as:

$$\mathbf{N} \frac{d\mathbf{x}}{dt} = \tilde{\mathbf{A}}\mathbf{x} + \mathbf{B}_u\mathbf{u} + \mathbf{B}_y\mathbf{y} \quad (3.7a)$$

$$\mathbf{y} = \tilde{\mathbf{C}}\mathbf{x} + \mathbf{D}_u\mathbf{u} + \mathbf{D}_y\mathbf{y} \quad (3.7b)$$

Where \mathbf{y} on the right side of the equations contains items associated with local inputs (as local outputs from other modules) and \mathbf{y} on the left side contains local outputs from the current module.

Procedures about how to establish the global steady-state equations are described in the

report [34]:

1. Break system into modules which represent a given operation or physical process.
2. Derive governing equations for each module.
3. By applying perturbation theory, collect first-order terms in the equations and ignore higher-order terms.
4. Discriminate the global and local inputs and write the equations in the format as equation 3.7.
5. Manipulate the equations into a global state-space format as equation 3.6.

A set of different coordinate systems have been defined in order to establish the module equations in step 2 and assemble the global equations in step 5, as shown in figure 3.2.

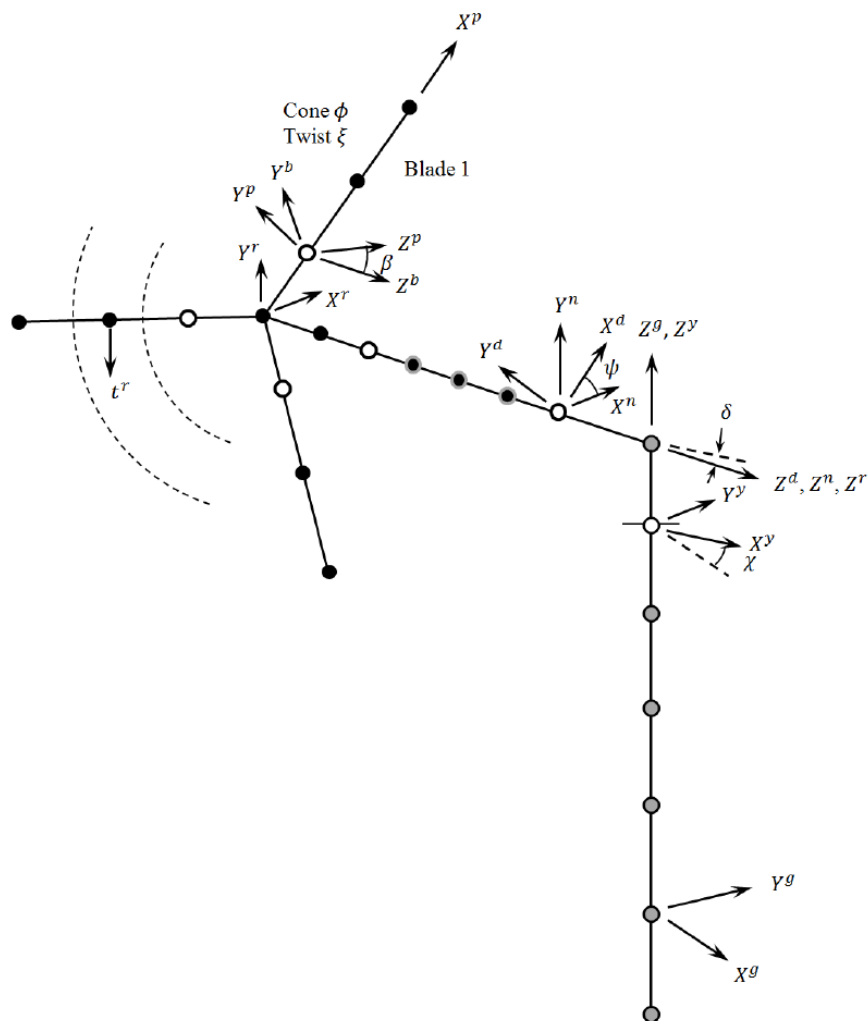


Figure 3.2: Coordinate systems used in the structural model [33]

Where the defined coordinate systems are:

- **g** : global coordinate system
- **y** : yaw coordinate system
- **n** : nacelle coordinate system
- **d** : drive-shaft coordinate system
- **r** : rotor plane coordinate system
- **b** : blade coordinate system
- **p** : blade pitch coordinate system

The procedures to calculate aerodynamic loads are summarised as shown in the figure 3.3.

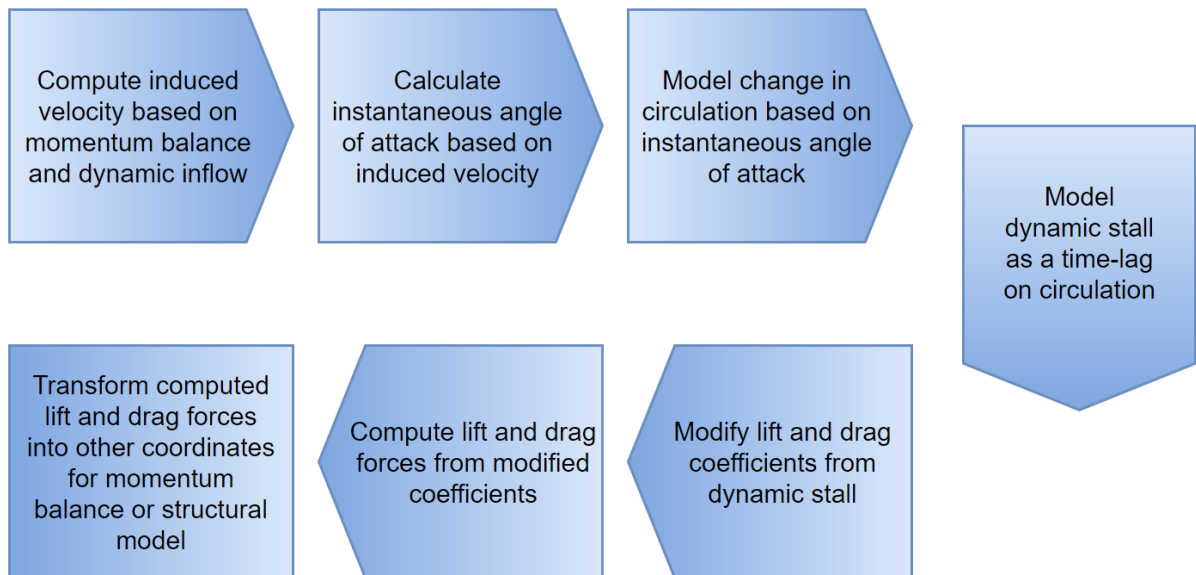


Figure 3.3: Procedures for calculating aerodynamic loads

In each step, linearizations have been applied and the resultant equations are transformed in the format of equation 3.7.

The non-linear terms in equation of motion are linearized based on the equation 3.8.

$$\mathbf{g}(\mathbf{x}, \dot{\mathbf{x}}, \ddot{\mathbf{x}}) \approx \mathbf{g}(\mathbf{x}_0, \dot{\mathbf{x}}_0, \ddot{\mathbf{x}}_0) + \left(\Delta \mathbf{x}^T \frac{\partial}{\partial \mathbf{x}} \Big|_0 + \Delta \dot{\mathbf{x}}^T \frac{\partial}{\partial \dot{\mathbf{x}}} \Big|_0 + \Delta \ddot{\mathbf{x}}^T \frac{\partial}{\partial \ddot{\mathbf{x}}} \Big|_0 \right) \mathbf{g} + \mathbf{O}(\Delta \mathbf{x}^2, \Delta \dot{\mathbf{x}}^2, \Delta \ddot{\mathbf{x}}^2) \quad (3.8)$$

Where \mathbf{g} is an arbitrary function and the operator $\partial/\partial s|_0$ is defined as 'first take the derivative with respect to s , then evaluate this at the steady-state condition' [34]. With equation 3.8, the total equation of motion can be linearized and some terms in each individual component are ignored due to small displacement assumptions.

By performing all the procedures mentioned above, the final linearized equation of motion is obtained.

$$\begin{aligned}
 (\mathbf{G}_M^B + \tilde{\mathbf{M}}_0^B) \frac{d^2 \Delta \mathbf{q}^B}{dt^2} = & \tilde{\mathbf{F}}_0^B - \mathbf{G}_{\Omega_0}^B - (\mathbf{G}_{\mathbf{K}_0}^B + \tilde{\mathbf{K}}^B) \mathbf{q}_0^B + \\
 & \Delta \tilde{\mathbf{F}}^B - (\mathbf{G}_C^B + \tilde{\mathbf{C}}^B) \frac{d \Delta \mathbf{q}^B}{dt} - (\mathbf{G}_K^B + \tilde{\mathbf{K}}^B) \Delta \mathbf{q}^B
 \end{aligned} \quad (3.9)$$

Where:

- Ω_0 is the mean rotational speed.
- $\mathbf{G}_{\mathbf{K}_0}^B$ represents steady-state terms which are dependent on Ω_0 and multiply q_0^B .
- $\mathbf{G}_{\Omega_0}^B$ represents the remainder of the steady-state terms which are depend upon Ω_0 .
- \mathbf{G}_C^B represents terms which are dependent on Ω_0 and multiply fluctuations in velocity.
- \mathbf{G}_K^B represents terms which are dependent on Ω_0 and multiply fluctuations in position.
- \mathbf{G}_M^B represents the rotational acceleration terms

The governing equation written in the format of equation 3.6 can be solved in both frequency domain and time domain. In frequency domain, transfer functions for interested parameters can be computed [34].

A linearized wind turbine model, based on the NREL 5MW reference wind turbine, has been provided by Karl Merz. After linearization, the state-space equation of motion for the wind turbine model has been sorted in a similar format as equation 3.4. To be connected together with the floater, the wind turbine states have been divided into two parts: the states of foundation reference node F (6 states describe motions and 6 states describe velocities) and the rest structural states of wind turbine, marked as T . Then the linear governing equation can be written as:

$$\begin{bmatrix} \mathbf{N}_{\text{TT}} & \mathbf{N}_{\text{TF}} \\ \mathbf{N}_{\text{FT}} & \mathbf{N}_{\text{FF}} \end{bmatrix} \frac{d}{dt} \begin{bmatrix} \Delta \mathbf{x}_{\text{T}} \\ \Delta \mathbf{x}_{\text{F}} \end{bmatrix} = \begin{bmatrix} \mathbf{A}_{\text{TT}} & \mathbf{A}_{\text{TF}} \\ \mathbf{A}_{\text{FT}} & \mathbf{A}_{\text{FF}} \end{bmatrix} \begin{bmatrix} \Delta \mathbf{x}_{\text{T}} \\ \Delta \mathbf{x}_{\text{F}} \end{bmatrix} + \begin{bmatrix} \mathbf{B}_{\text{T}} \\ \mathbf{B}_{\text{F}} \end{bmatrix} \Delta u(t) \quad (3.10)$$

Where:

- \mathbf{x}_{F} is the states of foundation reference node.
- \mathbf{x}_{T} is the rest structural states of the wind turbine.
- $u(t)$ is the wind speed.

3.3 Floater and wind turbine coupling

The linear state-space equations for floater and wind turbine have been developed in section 3.1 and section 3.2 respectively. To connect these two parts together, constraint equations need to be implemented between the foundation reference node F and the platform reference node P . In this section, how the constraint relationships are established will be discussed. The procedures performed here is based on a method developed by Karl Merz [33].

Since the platform is considered as a rigid body in this project, there is no platform deformation. This eliminates some terms with respect to node n in the original equations.

The notation which is applied in this section is defined as:

- $\mathbf{V}_{\mathbf{a}}^{\mathbf{B}}$: indicates a vector \mathbf{V} which is measured relative to the coordinate system a and the components of vector \mathbf{V} are expressed in the basis of coordinate system B .
- $\mathbf{T}_{\mathbf{a}}^{\mathbf{B}}$: indicates the transform matrix which transforms the vector expression basis from coordinate system a to coordinate system B .

In this section, coordinate systems defined are global coordinate system (g), operating point coordinate systems ($P0, F0, \dots$) and actual coordinate systems (P, F, \dots).

The states of the foundation reference node is expressed as:

$$\mathbf{X}_{\text{F}} = [\mathbf{O}_{\text{F}/g}^g \quad \Phi_{\text{F}}^{\text{F0}} \quad \mathbf{dO}_{\text{F}/g}^g/dt \quad \mathbf{d}\Phi_{\text{F}}^{\text{F0}}/dt]^T \quad (3.11)$$

Where:

- \mathbf{g} refers to the global coordinate system.
- $\mathbf{F0}$ refers to the coordinate system defined by the selected operating point.
- $\mathbf{O}_{F/g}^g$ is the vector of nodal position F .
- Φ_F^{F0} refers to the transform matrix \mathbf{T}_F^{F0} , which defines the rotation of node F . The transform matrix \mathbf{T}_F^{F0} can be written as a function of Φ_F^{F0} , that is $\mathbf{T}_F^{F0}(\Phi_F^{F0})$.

Similarly, the states of the platform reference node P is expressed as:

$$\mathbf{X}_P = [\mathbf{O}_{P/g}^g \quad \Phi_P^{P0} \quad d\mathbf{O}_{P/g}^g/dt \quad d\Phi_P^{P0}/dt]^T \quad (3.12)$$

From Spong et al [35], the transform matrix \mathbf{T}_{P0}^g is defined as:

$$\mathbf{T}_{P0}^g = \mathbf{R}_z(\theta_{P0z}) \mathbf{R}_y(\theta_{P0y}) \mathbf{R}_x(\theta_{P0x}) \quad (3.13)$$

Where:

$$\Phi_{P0}^g = [\theta_{P0x} \quad \theta_{P0y} \quad \theta_{P0z}]^T \quad (3.14)$$

$$\mathbf{R}_x(\theta_{P0x}) = \begin{bmatrix} 1 & 0 & 0 \\ 0 & \cos(\theta_{P0x}) & -\sin(\theta_{P0x}) \\ 0 & \sin(\theta_{P0x}) & \cos(\theta_{P0x}) \end{bmatrix} \quad (3.15)$$

$$\mathbf{R}_y(\theta_{P0y}) = \begin{bmatrix} \cos(\theta_{P0y}) & 0 & \sin(\theta_{P0y}) \\ 0 & 1 & 0 \\ -\sin(\theta_{P0y}) & 0 & \cos(\theta_{P0y}) \end{bmatrix} \quad (3.16)$$

$$\mathbf{R}_z(\theta_{P0z}) = \begin{bmatrix} \cos(\theta_{P0z}) & -\sin(\theta_{P0z}) & 0 \\ \sin(\theta_{P0z}) & \cos(\theta_{P0z}) & 0 \\ 0 & 0 & 1 \end{bmatrix} \quad (3.17)$$

Same method can be applied to compute the transform matrix \mathbf{T}_P^{P0} .

Then the three positional constraint relationships can be defined as:

$$\mathbf{O}_{P/g}^g + \mathbf{T}_P^g \mathbf{p}_{n/P}^P = \mathbf{O}_{F/g}^g \quad (3.18)$$

Where $\mathbf{p}_{n/P}^P$ is the vector of nodal position n .

Equation 3.18 describes that in the global coordinate system, the position of origin in foundation reference node coordinate system, is equal to the position of the platform connection node n plus the position of platform origin.

The three rotational constraint relationships are defined as:

$$\mathbf{T}_{P0}^g \mathbf{T}_P^{P0} \mathbf{T}_F^P \mathbf{T}_g^F = \mathbf{I} \quad (3.19)$$

Taking the first variation of equation 3.18 and equation 3.19 gives:

$$\delta \mathbf{O}_{P/g}^g + \left(\frac{\partial \mathbf{T}_P^g}{\partial \Phi_{P,k}^{P0}} \mathbf{p}_{n/P}^P \right) \delta \Phi_{P,k}^{P0} = \delta \mathbf{O}_{F/g}^g \quad (3.20)$$

and

$$\mathbf{T}_{P0}^g \frac{\partial \mathbf{T}_P^{P0}}{\partial \Phi_{P,k}^{P0}} \mathbf{T}_F^P \mathbf{T}_g^F \delta \Phi_{P,k}^{P0} + \mathbf{T}_F^g \frac{\partial \mathbf{T}_F^F}{\partial \Phi_{F,k}^{F0}} \delta \Phi_{F,k}^{F0} = \mathbf{0} \quad (3.21)$$

Where k in $\delta \Phi_{P,k}^{P0}$ has the value $k = 1, 2, 3$.

The rotation of the foundation reference node F is expressed with exponential map coordinates [32]. The relationship between an exponential map parameter θ_a^b and the transform

matrix T_a^b is expressed as:

$$[\theta_a^b]_{\times} := \ln \mathbf{T}_a^b = \begin{bmatrix} 0 & -\theta_{a,z}^b & \theta_{a,y}^b \\ \theta_{a,z}^b & 0 & -\theta_{a,x}^b \\ -\theta_{a,y}^b & \theta_{a,x}^b & 0 \end{bmatrix} \quad (3.22a)$$

$$\mathbf{T}_a^b = \exp [\theta_a^b]_{\times} \quad (3.22b)$$

Based on a simplified formula provided in Gallego and Yezzi [13], $\partial \mathbf{T}_a^b / \partial \theta_a^b$, the first order partial derivatives, are computed based on equation 3.23.

$$\frac{\partial \mathbf{T}_a^b}{\partial \theta_i} = \frac{\theta_i [\theta_a^b]_{\times} + [[\theta_a^b]_{\times} (\mathbf{I} - \mathbf{T}_a^b) \mathbf{e}_i]_{\times}}{\theta^T \theta} \mathbf{T}_a^b \quad (3.23)$$

Where \mathbf{e}_i is the i -th vector of the standard basis \mathbb{R}^3 .

In equation 3.21, the derivative in the second term is computed by:

$$\frac{\partial \mathbf{T}_g^F}{\partial \Phi_{F,k}^{F0}} = \frac{\partial \mathbf{T}_{F0}^F}{\partial \Phi_{F,k}^{F0}} \mathbf{T}_g^{F0} = \left(\frac{\partial \mathbf{T}_F^{F0}}{\partial \Phi_{F,k}^{F0}} \right)^T \mathbf{T}_g^{F0} \quad (3.24)$$

To write the constraint equations in state-space format, equation 3.20 is rewritten as:

$$\delta \mathbf{O}_{P/g}^g + \mathbf{E} \delta \Phi_P^{P0} = \delta \mathbf{O}_{F/g}^g \quad (3.25)$$

Where the 3×3 matrix \mathbf{E} is expressed as:

$$\mathbf{E} = \left[\frac{\partial \mathbf{T}_P^g}{\partial \Phi_{P,1}^{P0}} \mathbf{P}_{n/P}^P \quad \frac{\partial \mathbf{T}_P^g}{\partial \Phi_{P,2}^{P0}} \mathbf{P}_{n/P}^P \quad \frac{\partial \mathbf{T}_P^g}{\partial \Phi_{P,3}^{P0}} \mathbf{P}_{n/P}^P \right] \quad (3.26)$$

Same procedures have been applied to equation 3.21. The modulus in front of each state in equation 3.21 is a matrix rather than a vector. Since the matrices are skew-symmetric, three independent skew-symmetric terms (a_{12}, a_{13}, a_{23}) in each matrix are taken as the vector modulus for each state.

The resulting equation is expressed as:

$$\mathbf{G}\delta\Phi_P^{P0} + \mathbf{H}\delta\Phi_F^{F0} = \mathbf{0} \quad (3.27)$$

Where matrices \mathbf{G} and \mathbf{H} are 3×3 modulus matrices.

The equation 3.26 and equation 3.27 can be combined together as:

$$\mathbf{L}(\mathbf{q})\delta\mathbf{q} = \mathbf{0} \quad (3.28)$$

Where \mathbf{L} is a 6×12 matrix:

$$\mathbf{L} = \begin{bmatrix} \mathbf{I} & \mathbf{E} & -\mathbf{I} & \mathbf{0} \\ \mathbf{0} & \mathbf{G} & \mathbf{0} & \mathbf{H} \end{bmatrix} \quad (3.29)$$

and $\delta\mathbf{q}$ is the variation of states of node P and node F :

$$\delta\mathbf{q} = [\delta\mathbf{O}_{P/g}^g \quad \delta\Phi_P^{P0} \quad \delta\mathbf{O}_{F/g}^g \quad \delta\Phi_F^{F0}]^T \quad (3.30)$$

The relationship can also be derived as:

$$\mathbf{L}(\mathbf{q})\frac{d\mathbf{q}}{dt} = \mathbf{0} \quad (3.31)$$

From equation 3.28 and equation 3.31, totally 24 constraint relationships corresponding to the total 24 states of node P and node F have been established. Combine equation 3.28 and equation 3.31 together:

$$\begin{bmatrix} \tilde{\mathbf{L}}(\mathbf{q}) \\ \mathbf{L}(\mathbf{q})\frac{d\mathbf{q}}{dt} \end{bmatrix} = \mathbf{0} \quad (3.32)$$

Taking time derivatives of equation 3.32, the resulting equation can be written as:

$$\begin{bmatrix} \mathbf{L} & \mathbf{0} \\ \frac{\partial \mathbf{L}}{\partial \mathbf{q}} & \frac{d\mathbf{q}}{dt} \\ \frac{d\mathbf{q}}{dt} & \mathbf{L} \end{bmatrix} \frac{d}{dt} \begin{bmatrix} \mathbf{q} \\ \dot{\mathbf{q}} \end{bmatrix} = \mathbf{0} \quad (3.33)$$

The equation 3.33 expresses the constraint relationships between the states of node P and the states of node F . To be combined together with equation 3.5 and equation 3.10, the equation 3.33 is expanded to full states \mathbf{x}_t as in equation 3.34, where \mathbf{x}_t contains both floater states and wind turbine states.

$$\mathbf{K}(\mathbf{x}_t, \dot{\mathbf{x}}_t) \frac{d\mathbf{x}_t}{dt} = \mathbf{0} \quad (3.34)$$

Where \mathbf{x}_t is defined as:

$$\mathbf{x}_t = \begin{bmatrix} \mathbf{x}_T \\ \mathbf{x}_P \\ \mathbf{x}_F \end{bmatrix} = \begin{bmatrix} \hat{\mathbf{x}} \\ \mathbf{x}_F \end{bmatrix} \quad (3.35)$$

Since for a floating system with mooring system, the mean velocities associated with the states involved in constraint relationships are likely zero. The \mathbf{K} matrix after linearization will actually become a constant matrix [33]. So linearizing equation 3.32 and equation 3.34 at the operating point gives:

$$\mathbf{K}_0(\mathbf{x}_{t0}, \dot{\mathbf{x}}_{t0}) \Delta \mathbf{x}_t = \mathbf{0} \quad (3.36)$$

$$\mathbf{K}_0(\mathbf{x}_{t0}, \dot{\mathbf{x}}_{t0}) \frac{d\Delta \mathbf{x}_t}{dt} = \mathbf{0} \quad (3.37)$$

Separating the states of foundation reference node F in equation 3.36 gives:

$$\mathbf{K}_{F0} \Delta \mathbf{x}_F + \hat{\mathbf{K}}_0 \Delta \hat{\mathbf{x}} = \mathbf{0} \quad (3.38)$$

Solve $\Delta \mathbf{x}_F$ in equation 3.38:

$$\Delta \mathbf{x}_F = -\mathbf{K}_{F0}^{-1} \hat{\mathbf{K}}_0 \Delta \hat{\mathbf{x}} \quad (3.39)$$

From equation 3.39, the state reduction matrix Λ_0 is defined as:

$$\Lambda_0 := \begin{bmatrix} \mathbf{I} \\ -\mathbf{K}_{F0}^{-1} \hat{\mathbf{K}}_0 \end{bmatrix} \quad (3.40)$$

Which gives

$$\Delta \mathbf{x}_t = \Lambda_0 \Delta \hat{\mathbf{x}} \quad (3.41)$$

Similar relationship can be obtained from equation 3.37:

$$\frac{d\Delta \mathbf{x}_t}{dt} = \Lambda_0 \frac{d\Delta \hat{\mathbf{x}}}{dt} \quad (3.42)$$

Define the total input \mathbf{u} as:

$$\mathbf{u} := \begin{bmatrix} u(t) \\ \xi(t) \end{bmatrix} \quad (3.43)$$

Superposing equation 3.5 and equation 3.10 together gives:

$$\begin{bmatrix} \mathbf{N}_{TT} & \mathbf{0} & \mathbf{N}_{TF} \\ \mathbf{0} & \mathbf{N}_P & \mathbf{0} \\ \mathbf{N}_{FT} & \mathbf{0} & \mathbf{N}_{FF} \end{bmatrix} \frac{d\Delta \mathbf{x}_t}{dt} = \begin{bmatrix} \mathbf{A}_{TT} & \mathbf{0} & \mathbf{A}_{TF} \\ \mathbf{0} & \mathbf{A}_P & \mathbf{0} \\ \mathbf{A}_{FT} & \mathbf{0} & \mathbf{A}_{FF} \end{bmatrix} \Delta \mathbf{x}_t + \begin{bmatrix} \mathbf{B}_T \\ \mathbf{B}_P \\ \mathbf{B}_F \end{bmatrix} \Delta \mathbf{u} \quad (3.44)$$

Apply constraint relationships from equation 3.41 and equation 3.42:

$$\Lambda_0^T \begin{bmatrix} \mathbf{N}_{TT} & \mathbf{0} & \mathbf{N}_{TF} \\ \mathbf{0} & \mathbf{N}_P & \mathbf{0} \\ \mathbf{N}_{FT} & \mathbf{0} & \mathbf{N}_{FF} \end{bmatrix} \Lambda_0 \frac{d\Delta \hat{\mathbf{x}}}{dt} = \Lambda_0^T \begin{bmatrix} \mathbf{A}_{TT} & \mathbf{0} & \mathbf{A}_{TF} \\ \mathbf{0} & \mathbf{A}_P & \mathbf{0} \\ \mathbf{A}_{FT} & \mathbf{0} & \mathbf{A}_{FF} \end{bmatrix} \Lambda_0 \Delta \hat{\mathbf{x}} + \Lambda_0^T \begin{bmatrix} \mathbf{B}_T \\ \mathbf{B}_P \\ \mathbf{B}_F \end{bmatrix} \Delta \mathbf{u} \quad (3.45)$$

Equation 3.45 is the governing equation of motion for the combined wind turbine and floater

system. By applying constraint relationships and reducing the system states, the wind turbine model and floater model are coupled together.

3.4 Solve equation of motion in frequency domain

From section 3.3, the full linear model has been assembled together. To solve the equation of motion in frequency domain, the following procedures have been performed.

The governing equation of motion 3.45 can be expressed as:

$$\mathbf{N}_{\text{tot}} \frac{d\Delta\hat{\mathbf{x}}}{dt} = \mathbf{A}_{\text{tot}}\Delta\hat{\mathbf{x}} + \mathbf{B}_{\text{tot}}\Delta\mathbf{u} \quad (3.46)$$

Where in matrices \mathbf{N}_{tot} , \mathbf{A}_{tot} and \mathbf{B}_{tot} , frequency dependent terms are included.

Expressing equation 3.46 in frequency domain gives:

$$i\omega\mathbf{N}_{\text{tot}}\Delta\hat{\mathbf{x}} = \mathbf{A}_{\text{tot}}\Delta\hat{\mathbf{x}} + \mathbf{B}_{\text{tot}}\Delta\mathbf{u} \quad (3.47)$$

By solving the equation 3.47 in frequency domain, the total transfer functions from the inputs wind speed and wave elevation to global response are obtained.

$$\Delta\hat{\mathbf{x}} = [i\omega\mathbf{N}_{\text{tot}} - \mathbf{A}_{\text{tot}}]^{-1} \mathbf{B}_{\text{tot}}\Delta\mathbf{u} \quad (3.48)$$

That is:

$$\mathbf{H}_{\mathbf{uX}}(\omega) = [i\omega\mathbf{N}_{\text{tot}} - \mathbf{A}_{\text{tot}}]^{-1} \mathbf{B}_{\text{tot}} \quad (3.49)$$

3.5 Spectrum analysis

For turbulent wind and irregular waves, spectrum analyses have been applied in this project. Spectra of interested structural responses have been generated from linear dynamic model

in frequency domain. The corresponding time series from fully coupled time-domain simulations have been used to generate spectra. Then the spectra obtained from two different methods are compared in order to validate the developed linear dynamic model.

The response spectra from linear dynamic model can be expressed as:

$$\begin{aligned} \mathbf{S}_{\mathbf{X}\mathbf{X}}(\omega) &= \mathbf{S}_{\xi\xi}(\omega) |\mathbf{H}_{\xi\mathbf{X}}(\omega)|^2 + \mathbf{S}_{uu}(\omega) |\mathbf{H}_{\mathbf{u}\mathbf{X}}(\omega)|^2 \\ &= \mathbf{S}_{\xi\xi}(\omega) |\mathbf{H}_{\mathbf{F}_w\mathbf{X}}(\omega)|^2 |\mathbf{H}_{\xi\mathbf{F}_w}(\omega)|^2 + \mathbf{S}_{uu}(\omega) |\mathbf{H}_{\mathbf{F}_u\mathbf{X}}(\omega)|^2 |\mathbf{H}_{\mathbf{u}\mathbf{F}_u}(\omega)|^2 \end{aligned} \quad (3.50)$$

Where:

- $\mathbf{S}_{\mathbf{X}\mathbf{X}}$: the structural response spectrum.
- $\mathbf{S}_{\xi\xi}$: the wave spectrum.
- \mathbf{S}_{uu} : the wind speed spectrum.
- $\mathbf{H}_{\xi\mathbf{X}}$: the transfer function from wave elevation to structural response.
- $\mathbf{H}_{\mathbf{u}\mathbf{X}}$: the transfer function from wind speed to structural response.
- $\mathbf{H}_{\xi\mathbf{F}_w}$: the transfer function from wave elevation to hydrodynamic loads, which is the first order wave loads in this project.
- $\mathbf{H}_{\mathbf{F}_w\mathbf{X}}$: the transfer function from hydrodynamic loads to structural response.
- $\mathbf{H}_{\mathbf{u}\mathbf{F}_u}$: the transfer function from wind speed to wind loads acting on the structure.
- $\mathbf{H}_{\mathbf{F}_u\mathbf{X}}$: the transfer function from wind loads to structural response.

The time series of considered parameters have been read from time-domain simulation results. To obtain the spectra and compare with spectra from linear dynamic model, Fast Fourier Transform (FFT) have been performed based on the theory from Press et all [27].

The relationship between inputs and resulting parameters in a physical process can be described as a function in time domain or in frequency domain. Fourier transform allows the

transform between these two different expressions by:

$$Y(\omega) = \int_{-\infty}^{\infty} y(t)e^{i\omega t} dt \quad (3.51a)$$

$$y(t) = \frac{1}{2\pi} \int_{-\infty}^{\infty} Y(\omega)e^{-i\omega t} d\omega \quad (3.51b)$$

The spectrum used in structural analysis usually refers to the one-sided power spectrum, which is generated based on one-sided power spectral density (PSD):

$$P_y(\omega) = 2|Y(\omega)|^2 \quad (3.52)$$

The power spectral density can be obtained by performing Fourier transform to the function expressed in time domain and then following equation 3.52. Alternatively, based on Wiener-Khinchin theorem [27], one can compute the autocorrelation of the time-domain function first and then do the Fourier transform, which directly gives the power spectral density.

Since from time domain simulation, the time series data obtained is discretely sampled. Discrete Fourier transform should be applied. By equation 3.53, an approximation of continuous Fourier transform can be obtained from discrete Fourier transform.

$$Y(\omega_n) \approx \Delta Y_n \quad (3.53)$$

Where:

- $Y(\omega_n)$ is the continuous Fourier transform.
- Y_n is the discrete Fourier transform.
- Δ is the sampling interval, which usually refers to the time step in simulations.

In this project, function *dat2spec* in Wafo toolbox has been used in MATLAB scripts to generate the power spectrum density from time series data.

3.6 Eigenvalue problem

To validate that the linear dynamic model has right hydrodynamic characteristics, the structural natural periods in six DOFs are computed and compared with the results in Kvittem [23]. The natural frequencies can be obtained by solving general eigenvalue problem and computing the corresponding eigenfrequencies. It should be noticed that for the floater, it has frequency-dependent added mass. Direct iteration and inverse iteration have been applied to find the natural periods of the structure, based on theory in Langen and Sigbjornsson [24]. The highest eigenfrequency can be found by direct iteration. The lowest eigenfrequency can be found by inverse iteration and other eigenfrequencies can be found by inverse iteration with shift values.

The general eigenvalue problem for this model is expressed as:

$$(\mathbf{C} - \omega_i^2(\mathbf{M} + \mathbf{A}(\omega_i)))\Phi_i = \mathbf{0} \quad (3.54)$$

Where Φ_i refer to eigen vectors and ω_i are the corresponding eigenfrequencies.

Direct iteration

The iteration relationship is defined as:

$$\mathbf{Z}_k = (\mathbf{M} + \mathbf{A}(\omega))^{-1}\mathbf{C}\mathbf{Z}_{k-1} \quad (3.55)$$

Where \mathbf{Z}_k is the approximation to the eigen vector.

The eigenfrequency after convergence is computed by Rayleigh-quotient as:

$$\lambda_i = \omega_i^2 = \frac{\mathbf{Z}_k^T(\mathbf{M} + \mathbf{A}(\omega))\mathbf{Z}_k}{\mathbf{Z}_k^T(\mathbf{M} + \mathbf{A}(\omega))\mathbf{Z}_{k-1}} \quad (3.56)$$

Inverse iteration

The iteration relationship is defined as:

$$\mathbf{Z}_k = \mathbf{C}^{-1}(\mathbf{M} + \mathbf{A}(\omega))\mathbf{Z}_{k-1} \quad (3.57)$$

The corresponding eigenfrequency after convergence is computed by Rayleigh-quotient as:

$$\lambda_i = \omega_i^2 = \frac{\mathbf{Z}_k^T (\mathbf{M} + \mathbf{A}(\omega)) \mathbf{Z}_{k-1}}{\mathbf{Z}_k^T (\mathbf{M} + \mathbf{A}(\omega)) \mathbf{Z}_k} \quad (3.58)$$

For inverse iteration with a shift value u , the relationship is defined:

$$\lambda_i = u + \bar{\lambda}_i \quad (3.59)$$

Substituting equation 3.59 into equation 3.54 gives:

$$[(\mathbf{C} - u(\mathbf{M} + \mathbf{A}(\omega_i)) - \bar{\lambda}_i(\mathbf{M} + \mathbf{A}(\omega_i)))\Phi_i = \mathbf{0} \quad (3.60)$$

For the shifted eigenvalue problem, the iteration relationship is defined as:

$$\mathbf{Z}_k = (\mathbf{C} - u(\mathbf{M} + \mathbf{A}(\omega_i))^{-1}(\mathbf{M} + \mathbf{A}(\omega))\mathbf{Z}_{k-1} \quad (3.61)$$

The corresponding eigenfrequency after convergence is obtained as:

$$\lambda_i = \omega_i^2 = u + \frac{\mathbf{Z}_k^T (\mathbf{M} + \mathbf{A}(\omega)) \mathbf{Z}_{k-1}}{\mathbf{Z}_k^T (\mathbf{M} + \mathbf{A}(\omega)) \mathbf{Z}_k} \quad (3.62)$$

Chapter 4

Modelling and Procedures

In this chapter, the modelling work and procedures performed in this project will be presented. In section 4.1, the modified WindFloat design concept will be introduced. The loading conditions determined for this project will be explained in section 4.2. How the turbulent wind fields have been generated will be presented in section 4.3. The settings in time-domain simulations will be introduced in section 4.4. In the following section 4.5, how the linear dynamic model is assembled will be presented.

4.1 Modified WindFloat concept

The WindFloat design developed by Principle Power is shown in figure 4.1 [40]. In the original design, a 2.3 MW wind turbine has been mounted on a semi-submersible floater. The model used in this project has a 5 MW NREL reference wind turbine and is based on Roddier et al [30]. The model used in SIMA workbench (MARINTEK) is based on the work of Marit Kvittem [20] and provided by Professor Erin Bachynski at NTNU. To get desired stiffness, the mooring system developed by Marit Kvittem has slightly difference from Roddier et al [30]. Because of the difference in wind turbine capacity and mooring system, the concept design studied in this project is named as modified WindFloat by Professor Erin Bachynski.



Figure 4.1: The WindFloat design (without mooring system) [40]

The NREL 5MW reference wind turbine is developed by Jonkman et al as a reference to standardize the baseline offshore wind turbine specifications [19]. It is a conventional three-bladed upwind wind turbine with variable operating speeds and active blade pitch controller. Some of the important characteristics and design parameters of the NREL 5MW wind turbine are shown in the table 4.1.

Table 4.1: Design parameters of the NREL 5-MW wind turbine [19]

Parameter	Value	Unit
Rotor orientation	upwind	-
Rated power	5	MW
Number of blades	3	-
Rotor diameter	126	m
Hub diameter	3	m
Hub height	90	m
Rotor mass	110 000	kg
Nacelle mass	240 000	kg
Drivetrain	high speed, multiple-stage gearbox	-

Some important operation parameters of the NREL 5MW wind turbine are shown in table 4.2.

Table 4.2: Operation parameters of the NREL 5-MW wind turbine [19]

Parameter	Value	Unit
Cut-in wind speed	3.0	m/s
Rated wind speed	11.4	m/s
Cut-out wind speed	25.0	m/s
Cut-in rotor speed	6.9	rpm
Cut-out rotor speed	12.1	rpm

The original NREL 5MW wind turbine has a tower height of 87.6m [19]. Since the semi-submersible floater has a 10m structural extending above the sea water line (SWL), the tower height has been modified to 77.6m and the same tower properties as the tower developed for OC3-Hywind spar [16] have been implemented in the model.

The floater in WindFloat design has been used to support the NREL 5MW wind turbine in modified WindFloat concept. Some important parameters of the floater are presented in table 4.3 .

Table 4.3: Important parameters of the semi-submersible floater [20]

Parameter	Value	Unit
Mass	4019000	kg
Centre of gravity	(-4.3, 0.0, -7.9)	m
Number of columns	3	-
Column diameter	10.0	m
Operating draught	17.0	m
Airgap	10.0	m
Turbine tower foundation above SWL	10.0	m

As shown in figure 4.1, heave plates are designed at the bottom of each column to gain more damping and therefore, reduce the wave induced motions in heave direction. The three columns are mounted together by steel braces. The floater is positioned by four mooring lines, which have been redesigned by Marit Kvittem to get natural periods in horizontal plane

(surge, sway and yaw) close to the value specified in Roddier et al [30]. Two mooring lines are attached to the column where the wind turbine is mounted and one mooring line is attached to each of other two columns.

The natural periods of the modified WindFloat design concept are presented in table 4.4.

Table 4.4: Natural periods of the modified WindFloat design concept [20]

Surge	Sway	Heave	Roll	Pitch	Yaw
107.0s	124.8s	19.9s	35.6s	37.4s	68.5s

An active ballast system has been designed for the floater which will counteract the thrust force from rotor and keep the platform always floats upright [20]. This can be implemented in SIMA workbench (MARINTEK) by setting the mass coefficients as functions to wind speed. That is, for different mean wind speed applied, corresponding mass coefficients of the floater will be used in simulations and analyses. To be simplified, the active ballast system has not been considered in this project. The mass coefficients are simply defined to be the same as the value in zero mean wind speed condition.

4.2 Loading conditions

Based on the distribution data provided in Li et al [25], the loading conditions for the linear dynamic model and also time-domain simulations have been determined. First three wind speeds have been selected, one for below-rated, one for above-rated and one for extreme condition. For below-rated wind speed, 8 m/s has been selected. 18 m/s has been selected in above-rated condition. The significant wave height and peak period for a given wind speed are determined as most probable value in the marginal distribution. The distribution model developed in Li et al [25] have been used, following the same procedures as in Kristine [29].

For extreme condition, the value with a return period of 50 years have been used from Li et al [25]. Since in Li et al, hourly mean wind and wave hindcast data has been used as database to be fitted in distribution models. The probability of wind speed with a return period of 50 years can be computed as:

$$P(U > u_{50}) = \frac{1}{50 \lambda_n} \quad (4.1)$$

Where λ_n is the measurement intensity and for the distribution model used here, it is:

$$\lambda_n = 24 \times 365 = 8760$$

Substitute the resulting probability in the developed Weibull distribution model, the corresponding wind speed can be obtained. Same procedures can be followed to find the most probable significant wave height and peak period in extreme condition. As mentioned in section 2.1, the unidirectional wind and wave condition gives the most critical fatigue damage. Therefore, the turbulent wind and irregular waves are set to be unidirectional. The loading conditions are presented in table 4.5.

Table 4.5: Loading conditions determined for analyses [29]

Loading conditions	Below-rated	Above-rated	Extreme condition
Mean wind speed [m/s]	8.0	18.0	42.0
Significant wave height [m]	2.2	4.2	13.4
Wave peak period [s]	10.8	11.9	13.1

Since with turbulent wind, in order to maintain a constant power output, the pitch controller will start to work when the mean wind speed is above-rated. Therefore, for above-rated loading condition, pitch-controller needs to be implemented in the linear wind turbine model. In the extreme condition, the blades should be feathered and the wind turbine should be parked. Due to limited time, the linear dynamic model has been developed for below-rated loading condition only.

4.3 Turbulent wind field

Turbulent-wind simulator, TurbSim, has been used in this project to generate turbulent wind field for a given mean wind speed. The obtained turbulent wind fields have been applied in analyses for both linear dynamic model and time-domain simulations. As a statistical

model, TurbSim simulates time series of wind speed vectors numerically by applying Sandia method [17]. As shown in figure 4.2, the result files in TurbSim contain time series of three-component wind speed vectors for predefined grid points in a 2D vertical rectangular plane. The 2D vertical rectangular plane is fixed in the space.

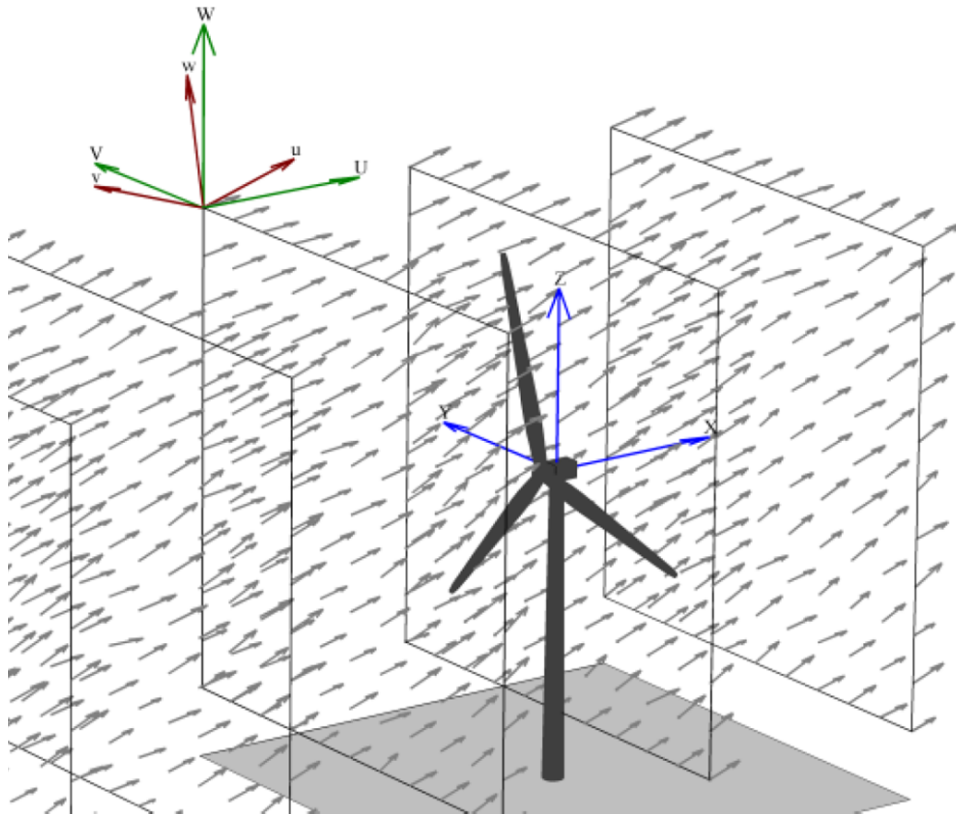


Figure 4.2: Turbulent wind field in TurbSim [17]

The wind speed time series are computed by applying inverse Fourier transform to the spectra of velocity components and spatial coherence defined in frequency domain [17]. To run the simulator, an input file needs to be selected based on different point-wind speed spectrum models. Then certain parameters in the input file need to be specified according to specific applications. The resulting output files can either be read in MATLAB or as inputs, be applied in other software. For offshore wind turbine, Kaimal spectral model is usually used as the point-wind speed spectrum model. The Kaimal spectral model is defined in the international standard IEC 61400-1 [7] where the expression of the model can be found. Some important parameter settings in Kaimal input file are presented and discussed in the following part.

- **RandSeed1, RandSeed2:** These two parameters are used to set the way for TurbSim to initialize the pseudorandom number generator (pRNG) [17].

The value for *RandSeed1* is specified as a random integer within a certain range. The value for *RandSeed2* can be either a random integer or a specific algorithm.

If the value of these two parameters are kept the same, the pRNG will be initialized in the same way, which means same random phases will be generated in different runs. In this project, different random numbers are given for these two parameters in order to get different wind field files.

- **WrBLFF :** is specified as 'true' to generate binary result files which can be imported in SIMA workbench (MARINTEK) as wind inputs.
- **GridHeight, GridWidth** define the size of the 2D vertical rectangular plane. The vertical rectangular plane should cover the rotor disk entirely. Considering the motion of floater and wind turbine, the size is set to be 160m × 160m.
- **NumGrid Z, NumGrid Y:** define the number of grid points in vertical and horizontal directions respectively. The recommended value is close to grid size divided by the mean chord of the turbine's blades [17]. The value does not need to be an even number, since TurbSim will always generate a point at hub. The data of this point at hub will not be included in the result file if an even number has been specified [17]. In this project, 32 points have been set in both directions, considering turbulence modelling and also the storage limit of the computer.
- **TimeStep, AnalysisTime, UsableTime:** TimeStep is defined in seconds, which determines the maximum frequency [17] by:

$$f_{max} = \frac{1}{\Delta t}$$

In this project, 0.05s is set as time step as recommended. The time length of analysis is set to be 3900s and data with a time length of 3600s has been used. Usable length of time series is set to be the same as the time length of analysis.

- **IECstandard** is set to be 3, which refers to international standard IEC 61400-3 (for off-shore wind turbine).

- **IECturbc, IEC WindType** IECturbc defines turbulence intensity used in wind speed spectral model. IECWindType indicates the IEC turbulence model applied. By setting these two parameters, the standard deviation and turbulence intensity of the longitudinal wind speed will be computed as a function of hub wind speed. In this project, IECturbc is set as 'B' and IEC WindType is set to be Normal Turbulence Model (NTM).
- **RefHt, URef** specify the reference height and reference wind speed. In this project, reference height is set to be 90m as the hub height and reference wind speed is set to be 8 m/s as in below-rated loading condition.
- **PLExp** defines the power-law exponent. Power-law wind profile is applied by setting value to this parameter[17]. Power-law wind profile is used to compute the mean longitudinal-component wind speeds across the rotor disk as shown below.

$$\bar{u}(z) = \bar{u}_{Ref} \left(\frac{z}{H_{Ref}} \right)^{PLExp}$$

In this project, the value is set to be 0.14. The resulting wind profile is shown in figure 4.3.

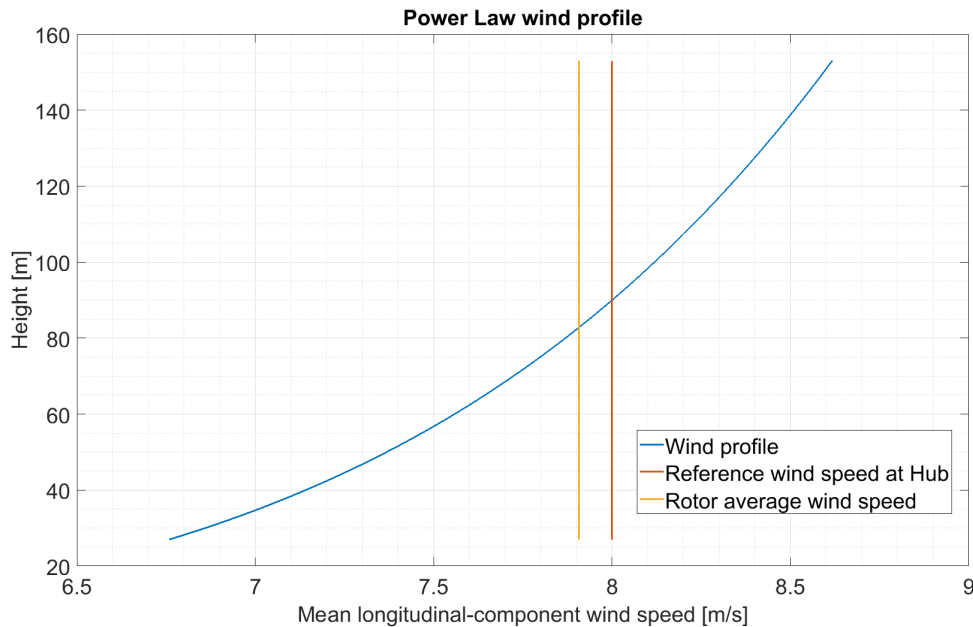


Figure 4.3: Power Law wind speed profile

A summary table of the parameter settings in TurbSim input file is presented in Appendix A. In this project, for a certain loading condition, only parameters **RandSeed1** and **RandSeed2**

have been changed in different run and other parameters have been kept the same. Totally 20 different turbulent wind fields have been simulated. Due to limited time, three of them have been used as inputs in time-domain simulations performed in SIMA workbench (MARINTEK).

4.4 Time-domain simulation

Fully-coupled time domain simulations have been run in SIMA workbench (MARINTEK) with environmental conditions specified in section 4.2. SIMA workbench is a software developed by MARINTEK based on SRA tool. The response is calculated by imposing dynamic equilibrium in each time step. The governing principle in SIMA is that the work done by external loads shall be equal to the work absorbed by the structure [31]. More theoretical details can be found in SIMO theory manual [31] and RIFLEX theory manual [28].

4.4.1 SIMA model

The model used in time domain simulations is provided by Professor Erin Bachynski at NTNU. A 3-D view of the SIMA model is shown in figure 4.4.

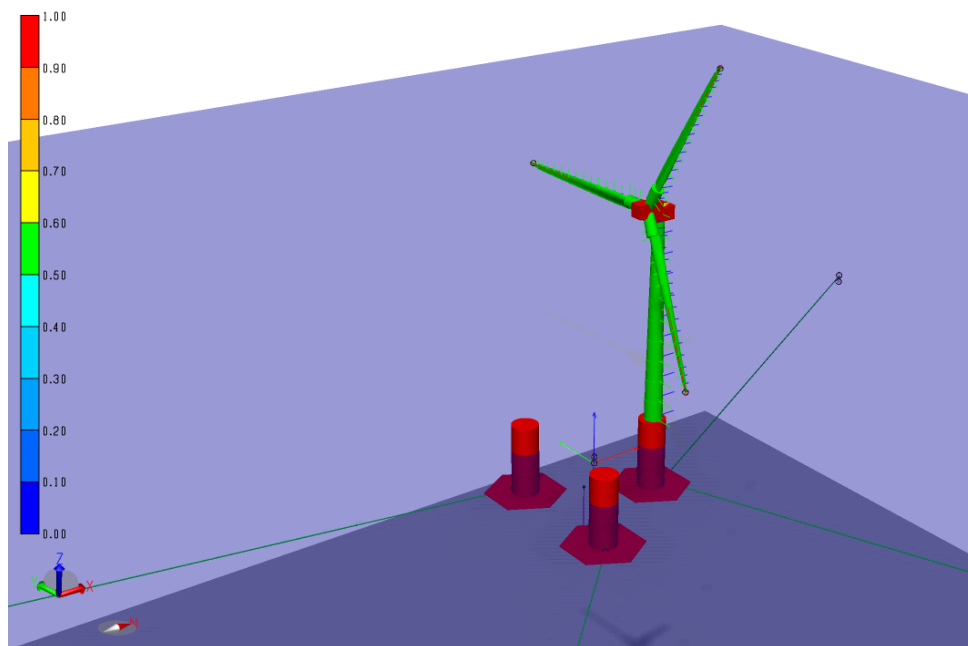


Figure 4.4: SIMA model used in time domain simulations

As shown in the figure 4.4, large volume structures are modelled as rigid SIMO bodies (with red colour), which include the floater, the wind turbine nacelle and the hub. Slender structures are modelled as flexible RIFLEX elements (with green colour), which include the wind turbine blades, the shaft, the tower and four mooring lines. The aerodynamic loads acting on the blades are calculated based on BEM with the Stig Øye correction for dynamic wake and the Stig Øye correction for dynamic stall [2].

4.4.2 Simulation and post-processing

For below-rated loading condition, totally 12 simulations with a simulation length 3900s for each have been run. Four random wave seeds have been set with significant wave height and peak period defined in the loading condition, and three turbulent wind fields generated by TurbSim have been imported as wind inputs, which gives 12 different combinations. The time step for result recording has been set as 0.05s, which is the same as in TurbSim. After setting relevant calculation parameters and parameters to be recorded, a condition set of 12 simulations have been run.

A set of MATLAB functions have been provided by Professor Erin Bachynski to read the simulation results from SIMA result files into MATLAB. These functions have been further implemented to consider all the results interested. The first 300s of the simulation is considered as transient stage and the corresponding data has been taken out from the time series. Spectrum analyses have been performed for the time series data. The mean platform motion and mean platform velocity have been computed as the operating point and used in the linearization of constraint equations.

For below-rated loading condition, four wave-only simulations have been run with different random wave seeds and no wind input. Three wind-only simulations have been run with different turbulent wind fields and a dummy wave input (significant wave height equals to 0.001m). Same post-processing procedures have been performed for wave-only and wind-only simulations.

SIMA simulations use different time vector for resulting time series. A table is presented in Appendix B to list time vectors used for different time series in this project.

4.5 Linear dynamic model

The linear dynamic model is developed as explained in chapter 3. The hydrodynamic model of the floater is assembled based on the WADAM analysis result from Kristine [29]. The modulus matrices of the linearized wind turbine model are provided by Karl Merz. To connect the floater and wind turbine together, constraint relationships have been established and linearized based on section 3.3. Spectrum analyses have been performed after the input wind and wave spectra have been generated.

4.5.1 Environmental input

To do the spectrum analysis in turbulent wind and irregular wave environmental condition, wind speed spectrum and wave spectrum are required as inputs, as shown in equation 3.50.

As mentioned in section 2.2, the site 14 located in the North Sea has been chosen. For North Sea operating condition, a Jonswap wave spectrum is generated with significant wave height and peak period specified by the loading condition. Same definition of the Jonswap spectrum in SIMA workbench (MARINTEK) has been applied [28]. The generated spectrum is shown in figure 4.5. Parameter settings of the wave spectrum are presented in Appendix C.

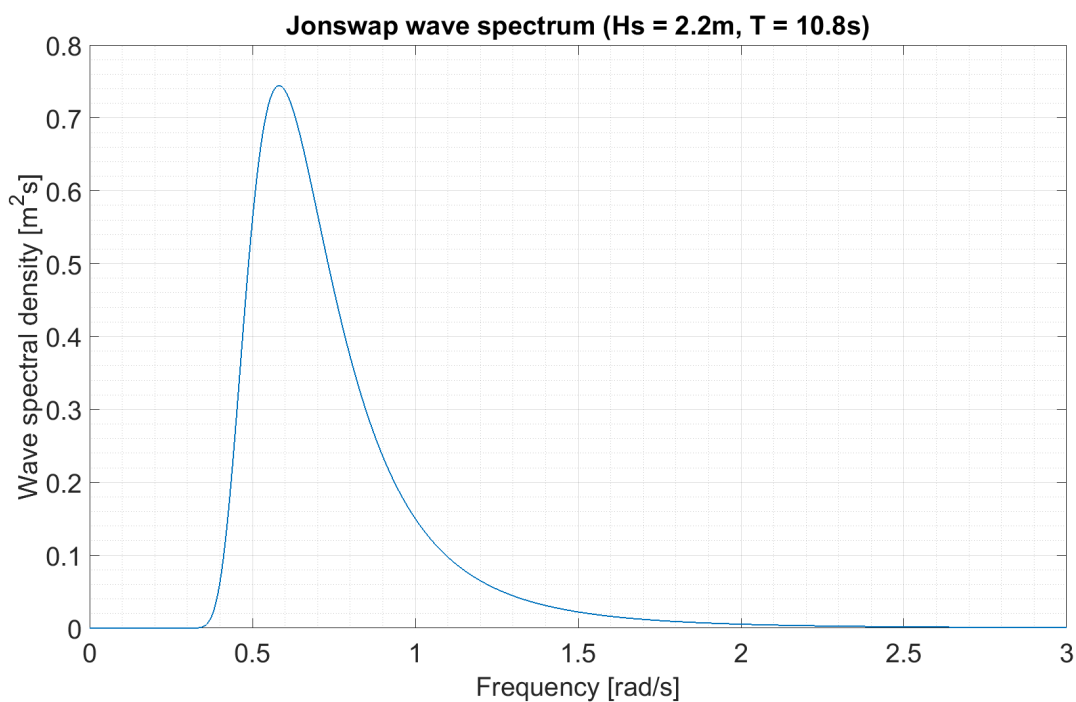


Figure 4.5: Jonswap wave spectrum

The linearized wind turbine model uses rotor-average wind speed spectrum as input. Therefore, rotor-average wind speed spectrum need to be generated. The result files of TurbSim simulations have been read in MATLAB, which gives data in a 4-D matrix. The four dimensions refer to time step, velocity component (u, v, w), y coordinate and z coordinate of the grid point. For each time step, the longitudinal wind speed components (u) of the grid points within the rotor disk have been averaged, which gives a time series of the rotor-average wind speed. Rotor-average wind speed spectra have been generated for those three TurbSim wind field files used in the time-domain simulations. These three spectra have been averaged and the averaged spectrum has been used as input for the linear dynamic model. The wind speed spectrum is shown in figure 4.6. Since the wind speed spectrum is narrow-band in low frequency range, it is plotted in log scale.

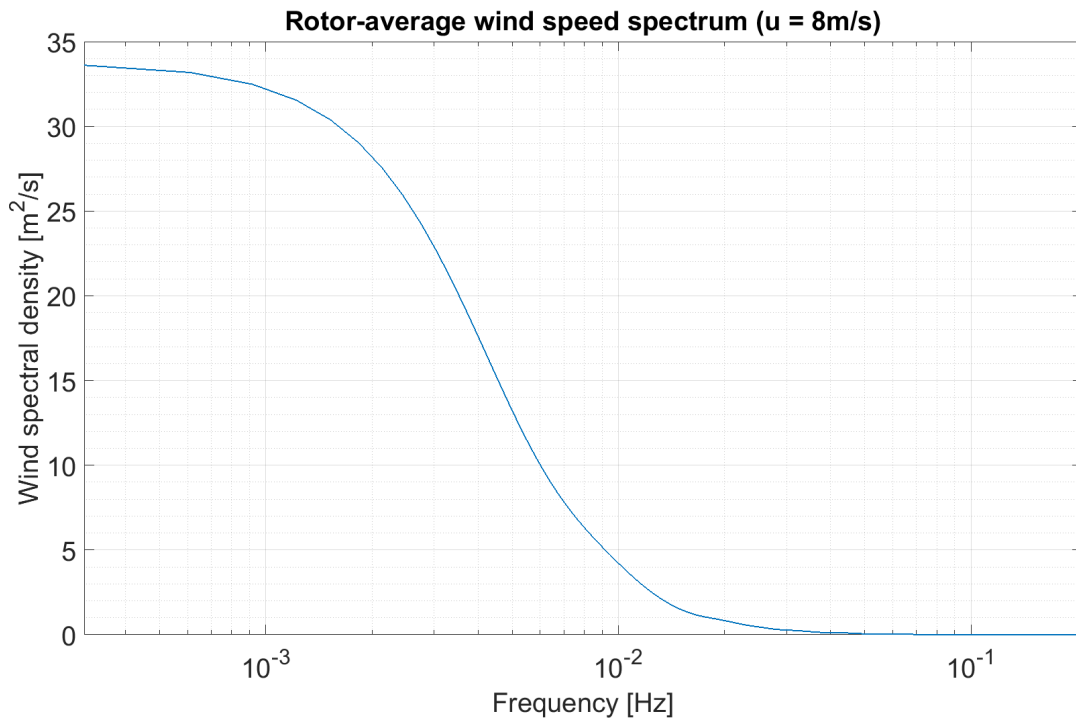


Figure 4.6: Rotor-average wind speed spectrum

4.5.2 Floater model

A result file of WADAM analysis is provided by Kristine [29], in which the hydrodynamic characteristics of the modified WindFloat concept are included. MATLAB scripts have been created to read this result file and sort the structural model matrices.

Mass matrix

Since in the WADAM result file, the mass coefficients (mass, centre of gravity and moment of inertia) are given for the whole structure, the mass coefficients of the floater itself are read from SIMA model. Based on Fossen [12], the mass matrix has been calculated for the floater.

$$\mathbf{M} = \begin{bmatrix} m & 0 & 0 & 0 & mz_g & -my_g \\ 0 & m & 0 & -mz_g & 0 & mx_g \\ 0 & 0 & m & my_g & -mx_g & 0 \\ 0 & -mz_g & my_g & I_x & -I_{xy} & -I_{xz} \\ mz_g & 0 & -mx_g & -I_{yx} & I_y & -I_{yz} \\ -my_g & mx_g & 0 & -I_{zx} & -I_{zy} & I_z \end{bmatrix} \quad (4.2)$$

Linear damping matrix

The linear damping matrix is read from the WADAM result file and assembled in MATLAB.

Linear stiffness matrix

The original linear stiffness matrix is read from the WADAM result file and assembled in MATLAB. The mooring system is not considered in the WADAM analyses made by Kristine. To consider the primary contribution on structural stiffness from mooring system, i.e. the horizontal stiffness, the mooring system is simplified as horizontal springs, as show in figure 3.1. The resulting spring stiffness have been added in the linear stiffness matrix.

To be simple, the structural motions in horizontal plane, i.e. in surge, sway and yaw directions, are assumed to be uncoupled. Then the hydrodynamic equation of motion of the structure can be simplified as shown in equation 4.3 where the subscript i refers to certain direction ($i = 1, 2, 6$ for surge, sway and yaw respectively).

$$[-\omega^2 (M_{ii} + A_{ii}(\omega)) + i\omega B_{ii}(\omega) + C_{ii}] x_i = f_i \quad (4.3)$$

By assuming the system is oscillating in a certain horizontal direction with corresponding natural frequency and the related damping term equals to zero, the equation 4.3 will be further simplified. By setting the wave excitation force f_i as zero, the equation becomes an general eigenvalue problem as shown in equation 4.4, in which ω_i refers to the natural fre-

quency in i direction and they can be obtained from natural periods in table 4.4.

$$[-\omega_i^2 (M_{ii} + A_{ii}(\omega_i)) + C_{ii}] x_{0i} = 0 \quad (4.4)$$

For the eigenvalue problem in equation 4.4, it is obvious that a solution exists when x_{0i} is not zero. That is:

$$-\omega_i^2 (M_{ii} + A_{ii}(\omega_i)) + C_{ii} = 0 \quad (4.5)$$

Therefore the mooring system stiffness C_{ii} can be obtained by solving equation 4.5 in the relevant horizontal directions and superposed to the corresponding elements in the linear stiffness matrix.

Since the influence of wind turbine on hydrodynamic stiffness has been considered in the wind turbine model, this part should be taken out from the linear stiffness matrix. This can be simplified by:

$$C_{44new} = C_{44} + m_{WT} g z_g \quad (4.6a)$$

$$C_{55new} = C_{55} + m_{WT} g z_g \quad (4.6b)$$

$$C_{46new} = C_{46} - m_{WT} g x_g \quad (4.6c)$$

$$C_{56new} = C_{56} - m_{WT} g y_g \quad (4.6d)$$

Where:

- m_{WT} is the mass of the wind turbine.
- x_g, y_g, z_g represent the centre of mass of the wind turbine.

Frequency-dependent terms

The frequency-dependent terms are frequency-dependent added mass matrix, frequency-

dependent damping matrix and first order wave load transfer functions. In WADAM analysis result file, the value of these terms are given for a set of sampling frequencies along the frequency range from 0 rad/s to 1.3 rad/s. MATLAB functions have been developed to compute the value of these frequency-dependent terms for given frequency inputs by interpolation or extrapolation.

4.5.3 Wind turbine model

The linearized NREL 5MW wind turbine model is provided by Karl Merz. The full aeroelastic matrices \mathbf{N} , \mathbf{A} and \mathbf{B} in equation 3.10 are linearized for an operating wind turbine at the mean wind speed of below-rated loading condition.

There are totally 493 states for the wind turbine model:

- **State 1-6:** Position and rotation states of the foundation reference node F .
- **State 7-78:** Other structural states.
- **State 79-84:** States as time derivatives of the position and rotation states of F .
- **State 85-156:** States as time derivatives of other structural states.
- **State 157:** The rotor speed.
- **State 158-493:** Aerodynamic states. 16 elements per blade and 7 states per blade element.

The linearized aeroelastic matrix files are read, assembled as matrices in MATLAB to be fitted in the full model.

4.5.4 Constraint equations

The constraint relationships described in section 3.3 have been implemented in MATLAB as a function, which requires the information of operating point to do linearization. The involved system states, i.e. the states of the foundation reference node F and the platform reference node P are set as symbolic variables. By implementing the value for these states at operating point and performing linearization, the resulting state reduction matrix Λ_0 can be computed and used as in equation 3.45.

4.5.5 Post-processing

By performing procedures described in section 3.3, the linear dynamic model is eventually developed. An illustration of the linear dynamic model is shown in figure 4.7.

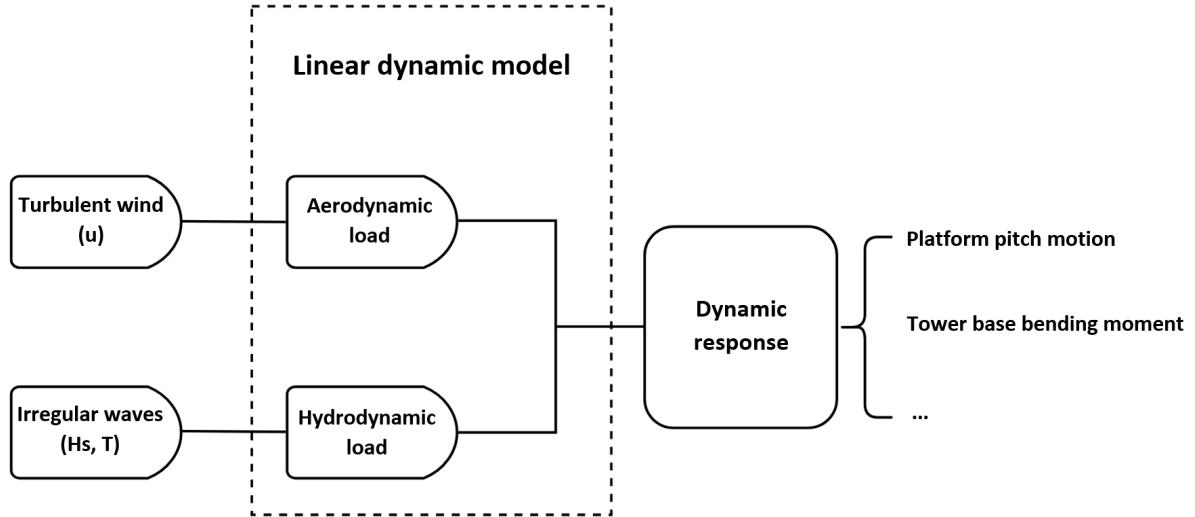


Figure 4.7: The developed linear dynamic model

The platform motion transfer functions have been computed. The transfer function from wave elevation to platform motion have been compared with the one obtained in the result file of WADAM analysis.

In addition, a modulus matrix \mathbf{C} of the linearized wind turbine model is provided by Karl Merz. This matrix has been expanded with floater states (a zero matrix). Then a similar state reduction procedure has been applied as shown in equation 4.7. The resulting matrix is the tower base bending moment transfer function as in equation 4.7, which has been used to compute the tower base bending moment in the linear dynamic model.

$$\mathbf{M} = \begin{bmatrix} \mathbf{C}_T & \mathbf{0} & \mathbf{C}_F \end{bmatrix} \Lambda_0 \Lambda_0^T \begin{bmatrix} \mathbf{x}_T \\ \mathbf{x}_P \\ \mathbf{x}_F \end{bmatrix} = \mathbf{C}_{\text{tot}} \hat{\mathbf{x}} = \mathbf{H}_{\text{uM}} \hat{\mathbf{x}} \quad (4.7)$$

The wind speed spectrum, wave spectrum, first order wave force spectra, platform pitch motion spectrum and tower base bending moment spectrum have been generated from the

linear dynamic model. They have been compared with the spectra obtained in time-domain simulations for wind-only, wave-only and combined conditions respectively.

Chapter 5

Results and comparison

By performing the procedures in chapter 4, the linear dynamic model for below-rated loading condition is developed. The results of dynamic response analysis have been computed by the linear dynamic model in frequency domain. They are listed in the following sections with comparison to the results obtained from fully coupled time-domain simulations.

5.1 Natural period comparison

The natural periods have been computed by performing the procedures in section 3.6. The value obtained is listed in table 5.1 with comparison to the results in Kvittem [23].

Table 5.1: Natural periods comparison

Direction	Method	Computed value [s]	Reference value [s][23]
Surge	Inverse+shift	107.04	107.0
Sway	Inverse	124.91	124.8
Heave	Direct	19.95	19.9
Pitch	Inverse+shift	37.48	37.4
Yaw	Inverse+shift	69.39	68.5

Where:

- **Direct** refers to direct iteration.

- **Inverse** refers to inverse iteration.
- **Inverse+shift** refers to inverse iteration with a shift value.

As shown in table 5.1, the value computed by iteration method is very close to the value in Kvittem [23].

Since the natural period in roll direction is very close to the value in pitch, as shown in table 4.4, the natural period in roll direction have not been obtained from iteration method. Because when applying a shift value close to the roll natural period, the iteration always converges to the pitch natural period.

5.2 Platform motion transfer function comparison

For combined wind and wave condition, the transfer functions from wave elevation to platform motion have been computed. They have been compared with the results from WADAM analysis. The results in surge, heave and pitch directions are shown in figure 5.1, figure 5.2 and figure 5.3 respectively.

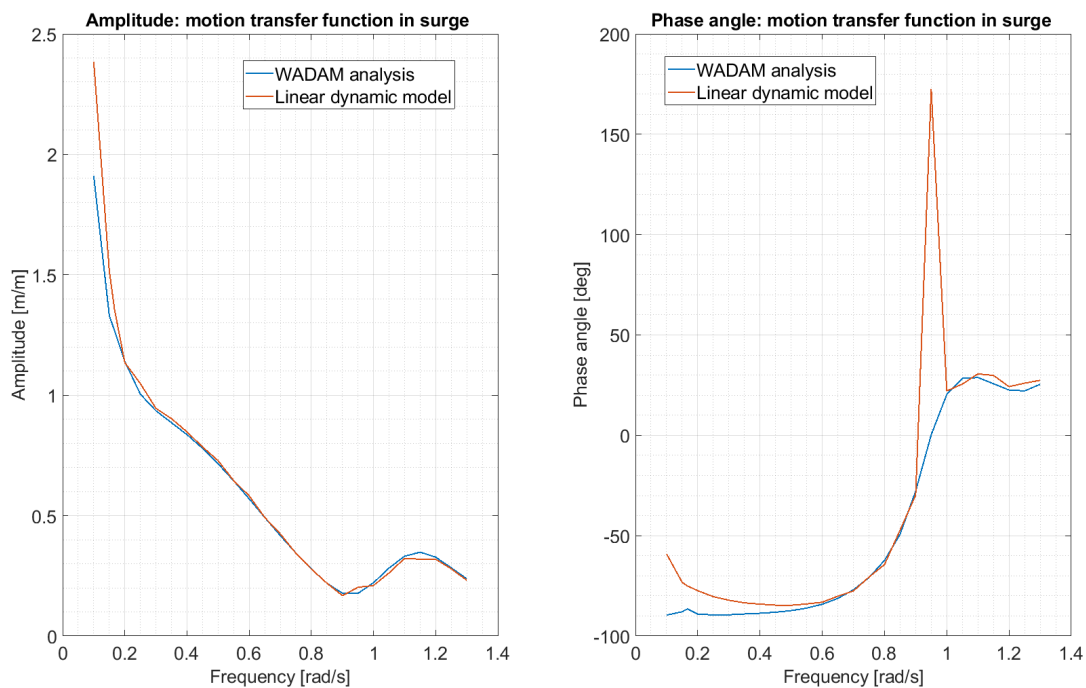


Figure 5.1: Transfer function from wave elevation to platform motion-surge

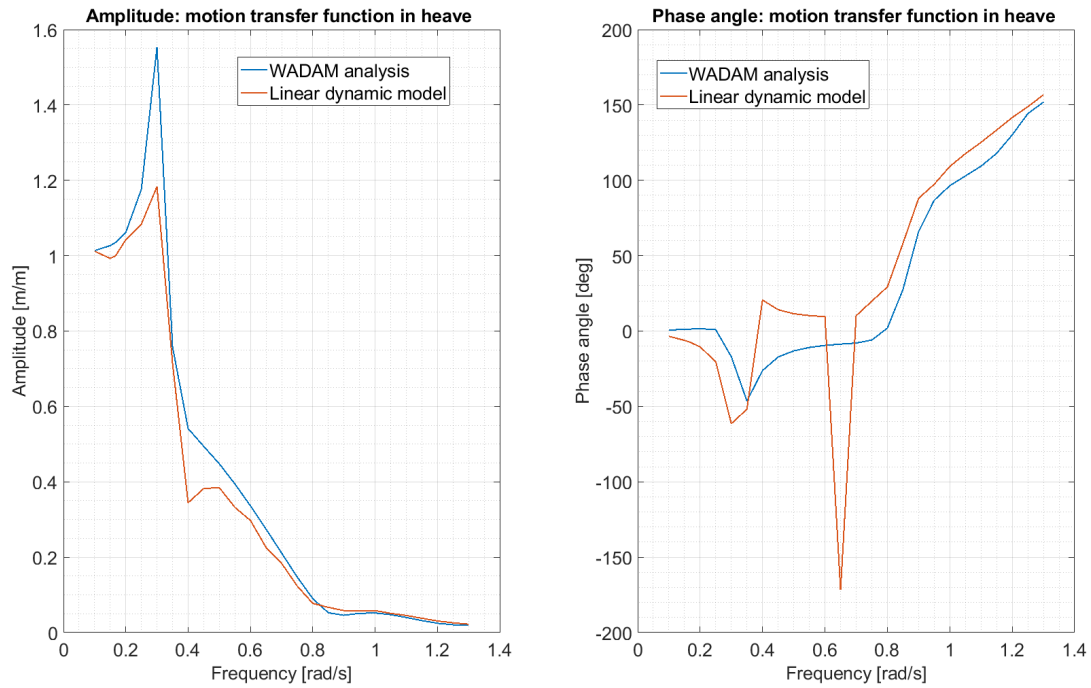


Figure 5.2: Transfer function from wave elevation to platform motion-heave

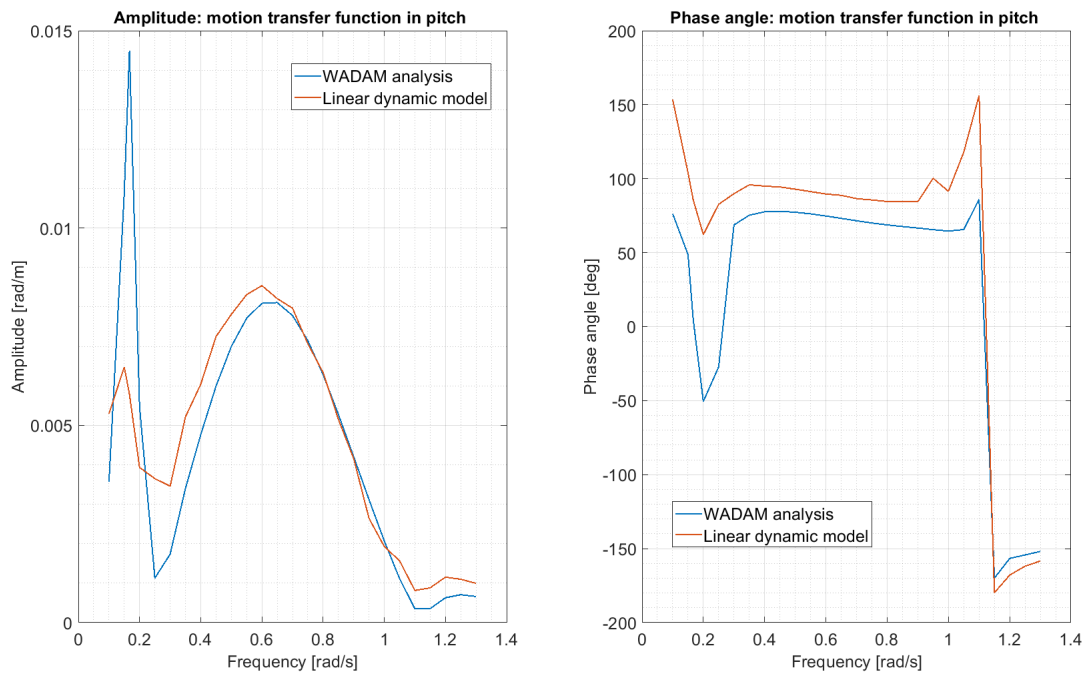


Figure 5.3: Transfer function from wave elevation to platform motion-pitch

From the amplitude plots, it can be observed that the value has a good agreement within the wave frequency range in figure 4.5, which is approximately from 0.4 rad/s to 1.3 rad/s. In the lower frequency range, they still have similar peak frequencies, but the peak value differ in

some degree. The phase angle plots show an agreement of the trend in general.

The amplitude of transfer function from wind speed to platform motion in pitch direction has been computed and plotted in figure 5.4. Some statistics are summarized in table 5.2.

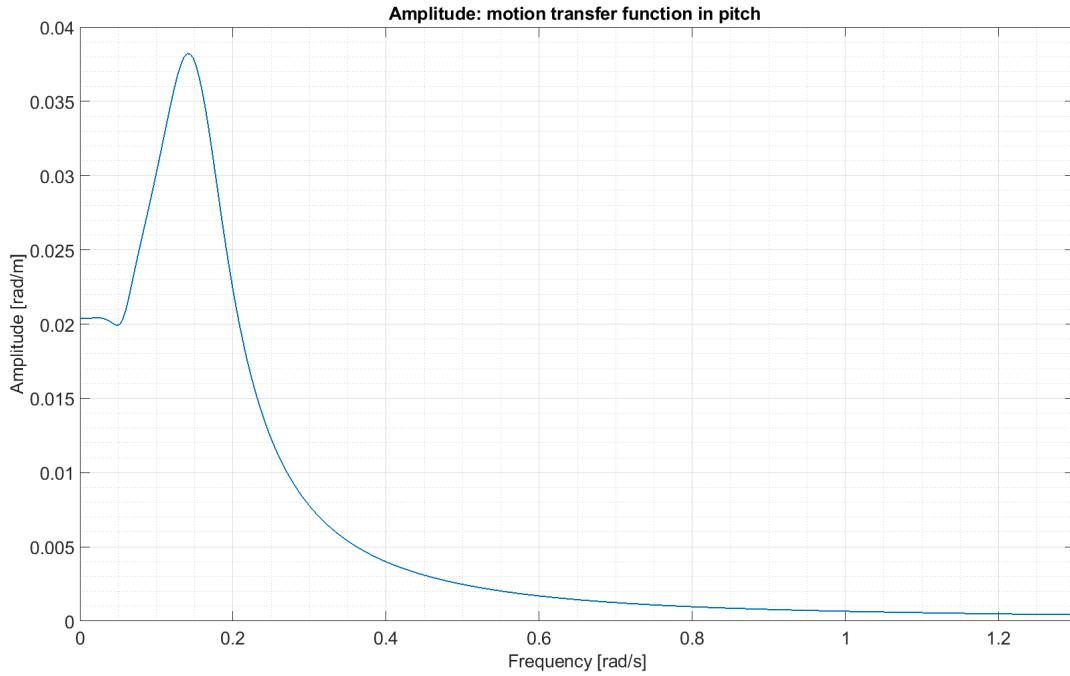


Figure 5.4: Transfer function from wind speed to platform motion-pitch

Table 5.2: Peak value in transfer function from wind speed to platform motion

Peak frequency	Peak amplitude	Amplitude at zero frequency
0.14 rad/s	0.03822 rad/m	0.02037 rad/m

From figure 5.4 it can be observed that the amplitude of pitch motion transfer function has a relatively stable value with an increasing frequency until it reaches 0.052 rad/s. A peak value can be found with frequency equals to 0.14 rad/s.

5.3 Spectrum analysis

5.3.1 Combined wind and wave condition

Following section 4.4.2, the generated spectra from 12 different time-domain simulations have been averaged and compared with the spectra obtained from linear dynamic model.

The wave spectra comparison is shown in figure 5.5. The standard deviations (STD) for both linear dynamic model and time-domain simulation have been computed and compared in table 5.3.

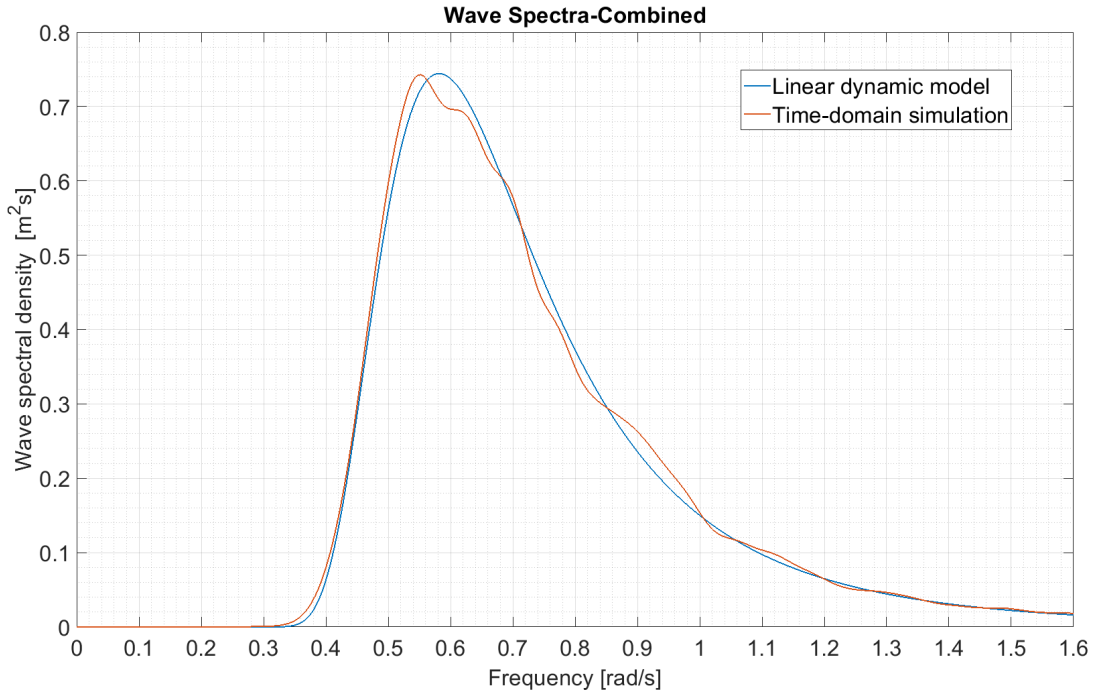


Figure 5.5: Wave spectra in combined condition

Table 5.3: Comparison: wave spectra-combined condition

Parameter	Linear dynamic model	Time-domain simulation	Error
STD	0.5439	0.5516	1.40 %

From figure 5.5 and table 5.3, a good agreement between the results from linear dynamic model and the results from time-domain simulations can be observed.

The wind speed spectra are shown in figure 5.6. For the linear dynamic model, as stated in section 4.5.1, the spectra have been generated and averaged from rotor-average wind speed time series. For time domain simulations, the spectra have been generated and averaged from the longitudinal wind speed time series at hub point. The standard deviations for both cases have been computed and presented in table 5.4. Since the spectra are narrow-band in the low-frequency range, as shown in figure 5.6, a log-scale version is presented in figure 5.7.

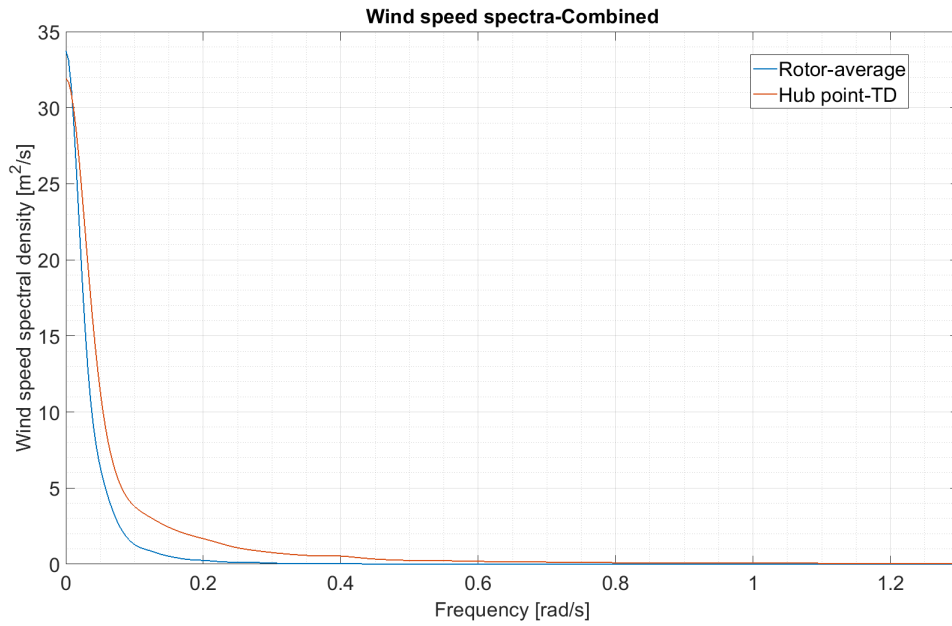


Figure 5.6: Wind speed spectra in combined condition

Table 5.4: Comparison: wind speed spectra-combined condition

Parameter	Linear dynamic model	Time-domain simulation	Difference
STD	1.0924	1.4358	23.92 %

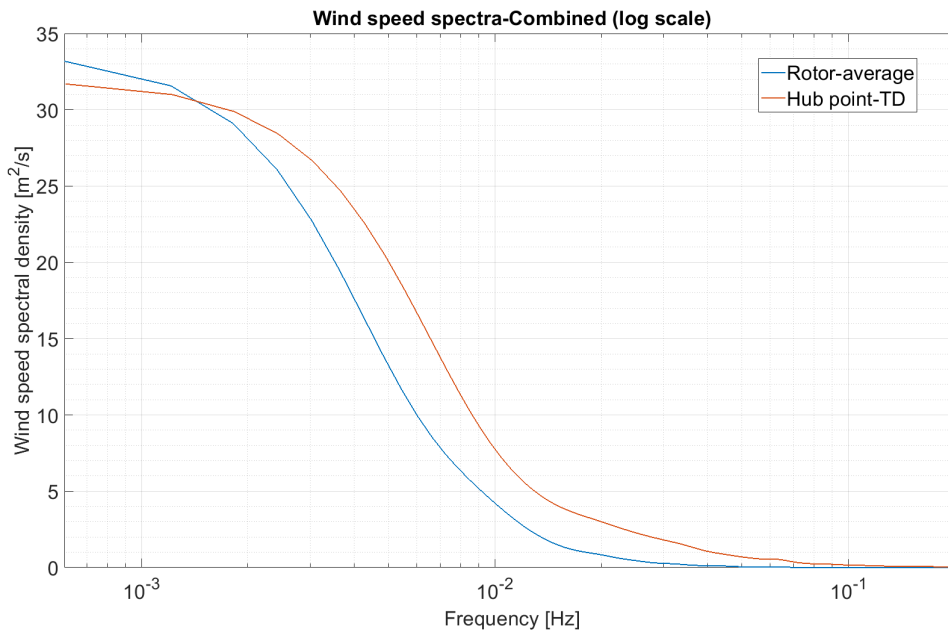


Figure 5.7: Wind speed spectra in combined condition (log scale)

As the wind speed spectra are generated from time series of different parameters, they are

not supposed to be the same theoretically. It can be observed that the rotor-average wind speed spectrum has a more narrower shape in low frequency range.

The wave force (first-order wave load in this project) spectra have been plotted and shown in figure 5.8. For wave forces, the results from linear dynamic model agrees well with time-domain simulation results in each direction. Double peaks are observed in surge wave force spectrum, which may due to the force cancellation considering the relationship between the wave length and the floater dimension.

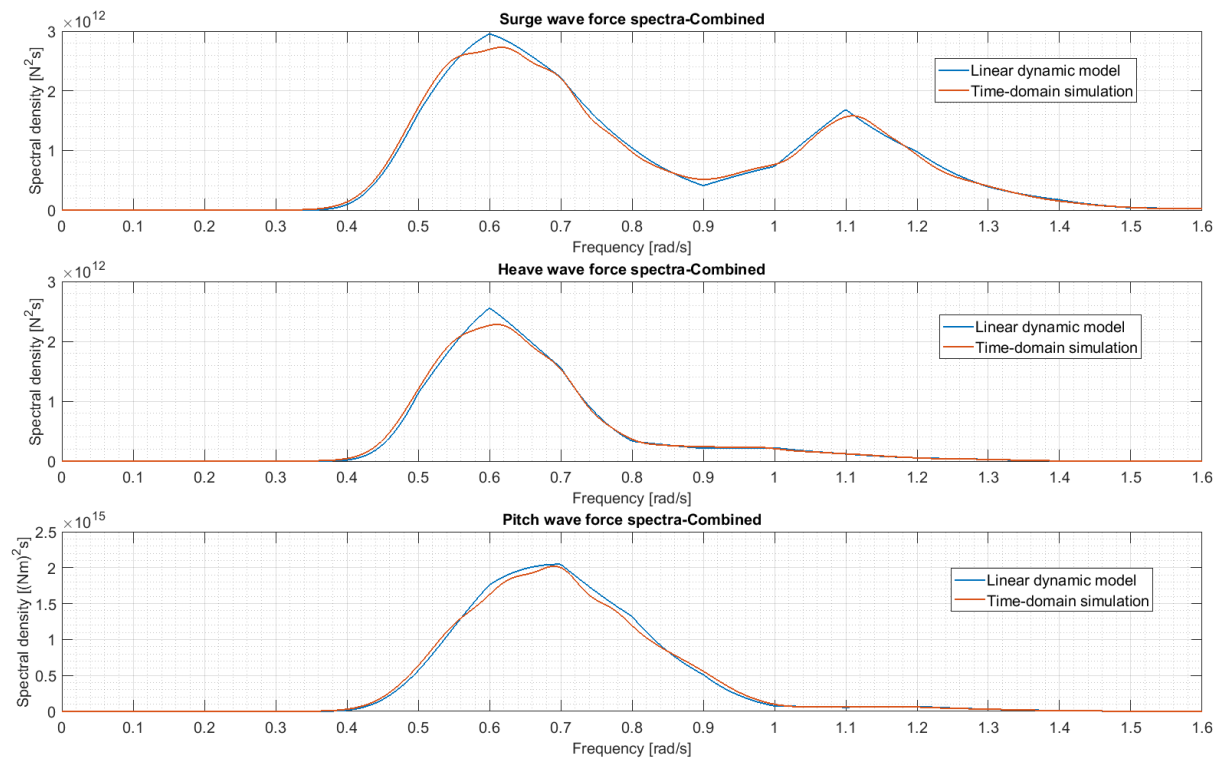


Figure 5.8: Wave force spectra in combined condition

The platform pitch motion response spectra have been computed and presented in figure 5.9. The standard deviations for both cases have been computed and presented in table 5.5. The mean value and standard deviation for time-domain simulations are computed directly from time series data, while the standard deviation for linear dynamic model is computed by taking the square root of the area under the spectrum density curve. As shown in figure 5.9, in the below-rated loading condition, the platform motion in pitch direction is mainly driven by wind load.

A log-scale version of the pitch motion response spectra is generated and presented in figure

5.10. It is clearer that the linear dynamic model underestimates the pitch motion response spectral density in low frequency range.

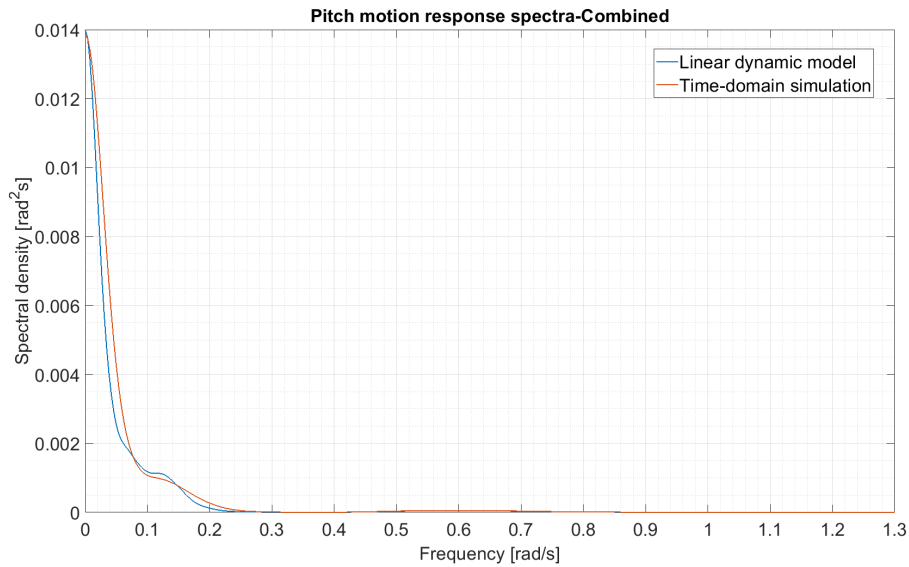


Figure 5.9: Pitch motion response spectra in combined condition

Table 5.5: Comparison: pitch motion response-combined condition

Parameter	Linear dynamic model	Time-domain simulation	Error
Mean pitch motion	-	0.1082 rad	-
STD	0.0238	0.0261	8.81 %

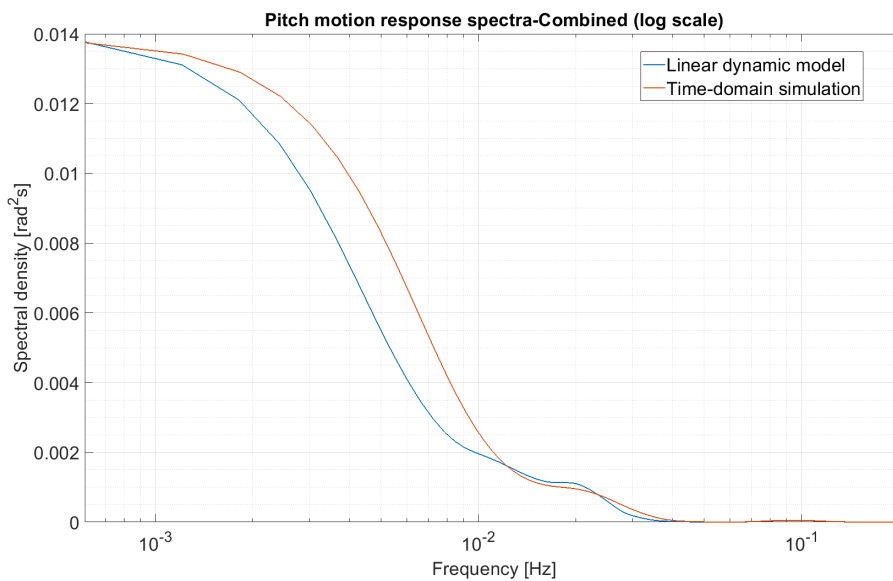


Figure 5.10: Pitch motion response spectra in combined condition (log scale)

The spectra comparison of tower base bending moment are shown in figure 5.11. The standard deviations for both cases have been computed and presented in table 5.6. The mean value and standard deviation for time-domain simulations are computed directly from time series data, while for linear dynamic model, the STD is computed by taking the square root of the area under spectrum density curve.

A log-scale version of the tower base bending moment spectra is presented in figure 5.12. It can be observed that the bending moment spectra follow a similar trend as in pitch motion spectra comparison. The linear dynamic model underestimates the spectral density of tower base bending moment. One part of the tower base bending moment comes from the gravity force of the wind turbine in pitch motion. Another part comes from thrust force acting on the rotor, which is initially caused by the aerodynamic loads acting on the wind turbine blades. This may explain that the error in tower bending moment comparison is larger.



Figure 5.11: Tower base bending moment spectra in combined condition

Table 5.6: Comparison: tower base bending moment-combined condition

Parameter	Linear dynamic model	Time-domain simulation	Error
Mean M_{TB}	-	7.0652e+07 Nm	-
STD	1.4947E+07	1.9084E+07	21.68 %

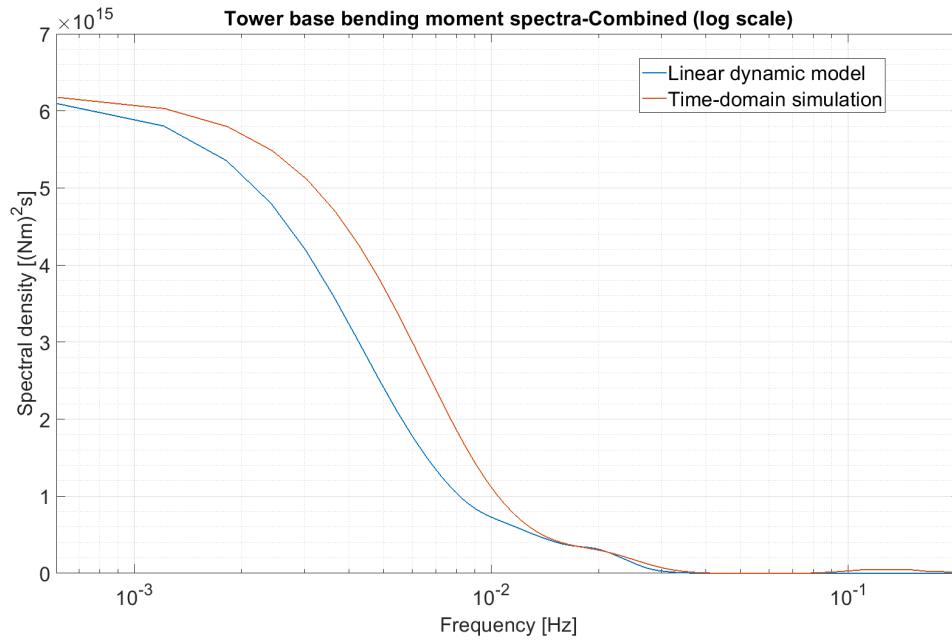


Figure 5.12: Tower base bending moment spectra in combined condition (log scale)

5.3.2 Wave only condition

The results from four wave-only time-domain simulations have been read in MATLAB with post-processing procedures described in section 4.4.2. The resulting spectra have been computed and compared with the spectra obtained from linear dynamic model. The comparison is presented in this section. Generally, a good agreement between the linear dynamic model and the time-domain simulations is shown in wave only condition.

The comparison of wave spectra is presented in figure 5.13. The standard deviations for both linear dynamic model and time-domain simulations have been computed and shown in table 5.7.

Table 5.7: Comparison: wave spectra-wave only condition

Parameter	Linear dynamic model	Time-domain simulation	Error
STD	0.5439	0.5516	1.40%

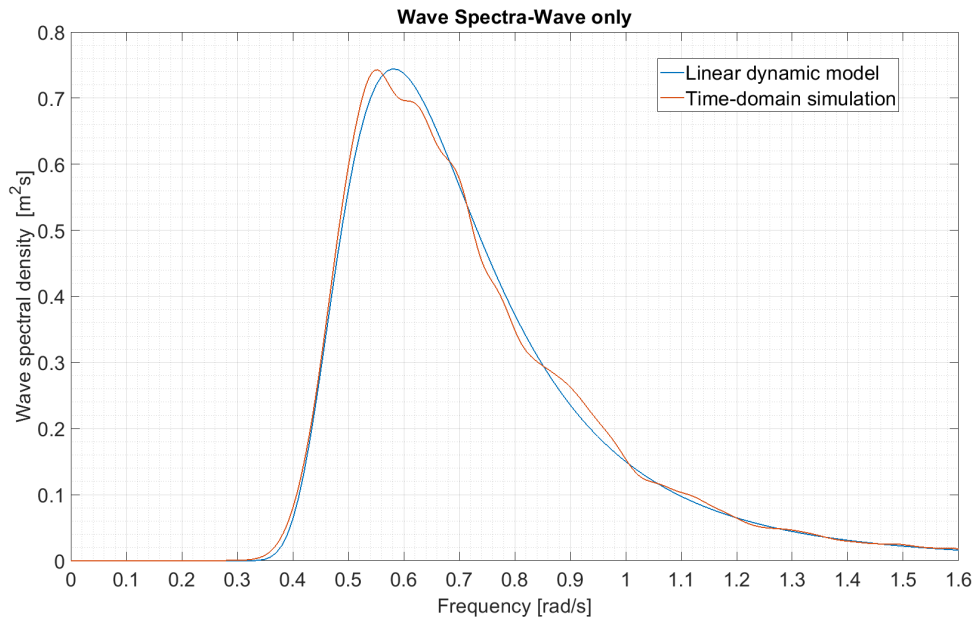


Figure 5.13: Wave spectra in wave only condition

The wave force spectra spectra have been plotted and shown in figure 5.14, in which a good agreement between the results from linear dynamic model and the time-domain simulation results can be observed.

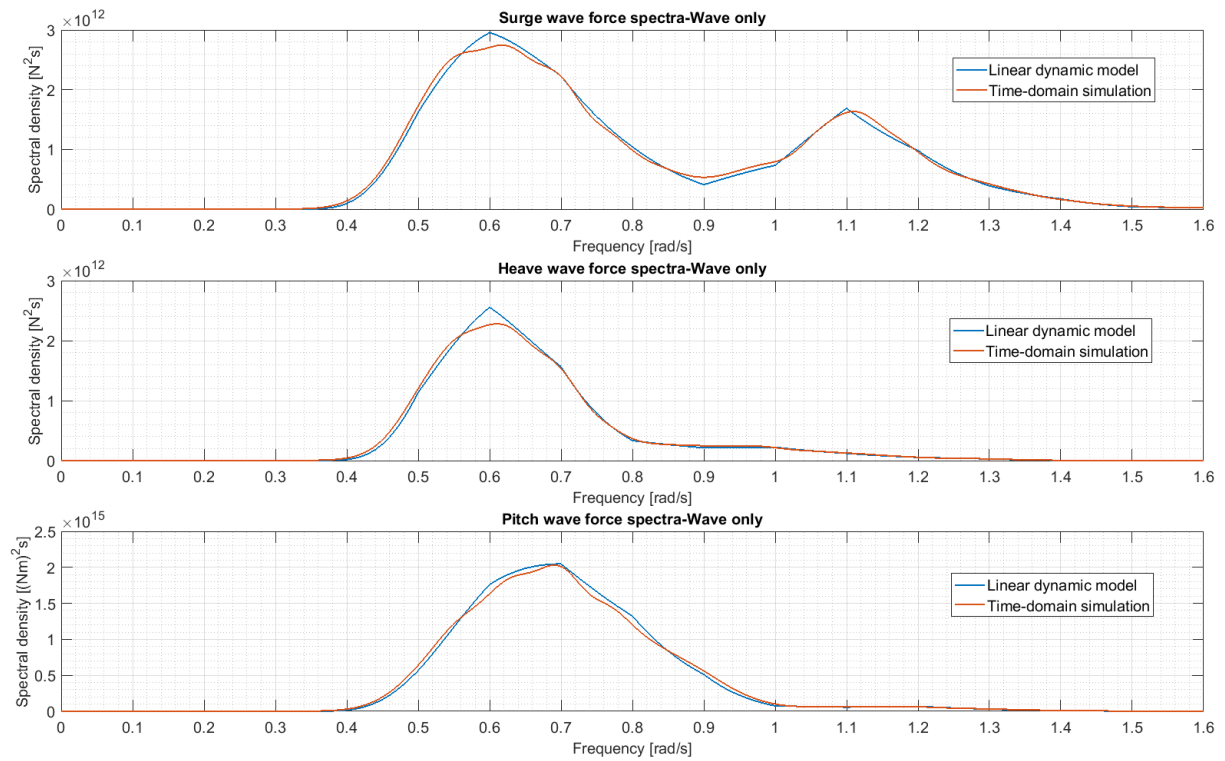


Figure 5.14: Wave force spectra in wave only condition

The platform pitch motion response spectra have been computed and presented in figure 5.15. It can be observed that results from linear dynamic model follows well with the results from time-domain simulations, except when the frequency is close to the peak frequency, where the linear dynamic model gives an overestimation.

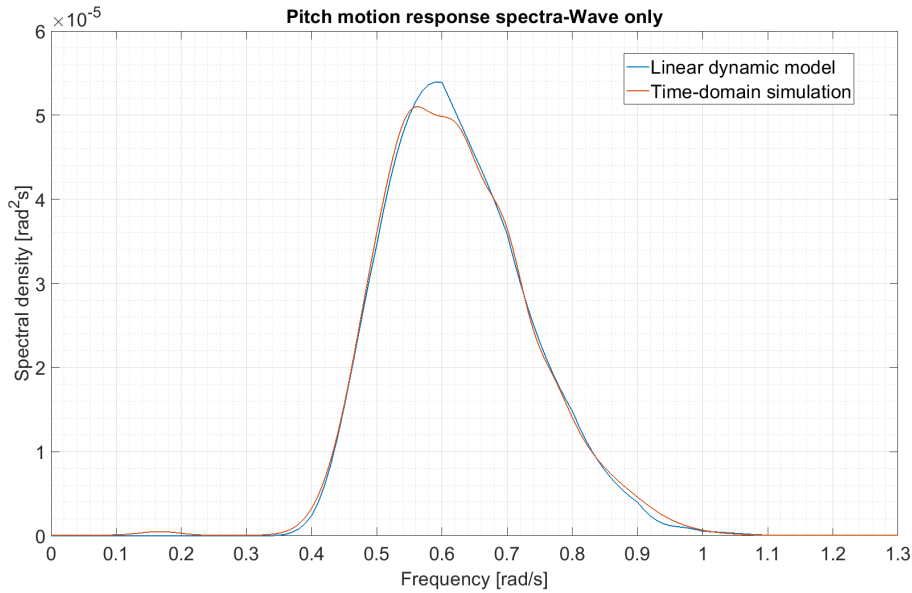


Figure 5.15: Pitch motion response spectra in wave only condition

The standard deviations for both cases have been calculated and presented in table 5.8. They have very close value. The mean value and standard deviation of the pitch motion in time-domain simulation are calculated directly from time series data.

Table 5.8: Comparison: pitch motion response spectra-wave only condition

Parameter	Linear dynamic model	Time-domain simulation	Error
Mean pitch motion	-	0.002 rad	-
STD	0.0038	0.0038	0 %

5.3.3 Wind only condition

The results from three wind-only time-domain simulations in SIMA workbench have been read in MATLAB and post-processing procedures have been performed as in section 4.4.2. The resulting spectra have been plotted together with the spectra obtained from the results

computed by linear dynamic model. The results follow similar trends, though an overall underestimation is shown in the results from linear dynamic model.

The wind speed spectra are shown in figure 5.16. The standard derivations for both cases have been calculated and presented in table 5.9. A log-scale version of the wind speed spectra is shown in figure 5.17.

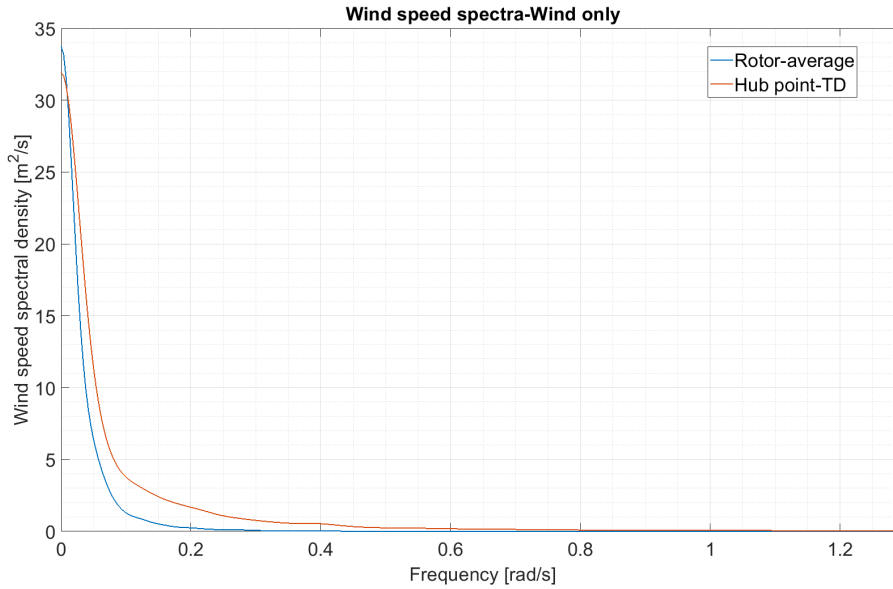


Figure 5.16: Wind speed spectra in wind only condition

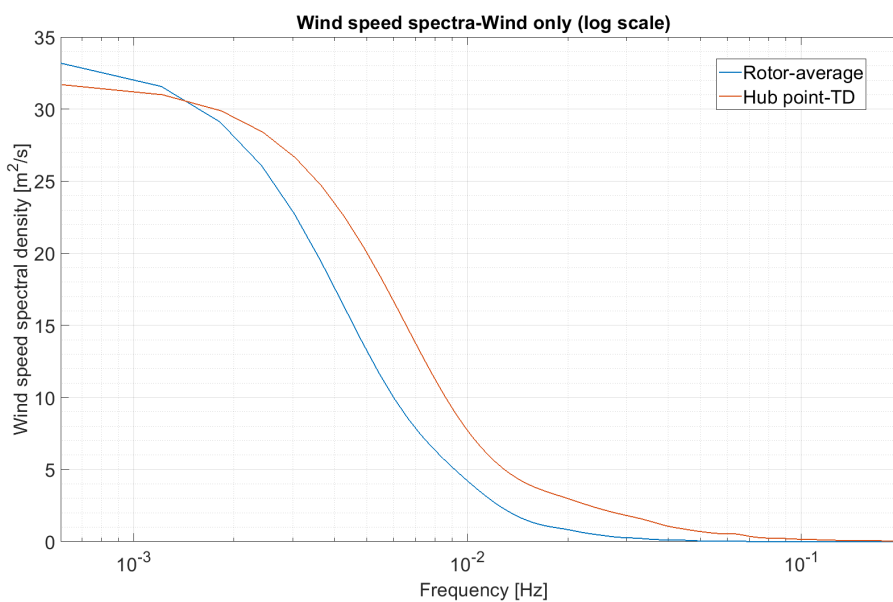


Figure 5.17: Wind speed spectra in wind only condition (log scale)

Table 5.9: Comparison: wind speed spectra-wind only condition

Parameter	Linear dynamic model	Time-domain simulation	Difference
STD	1.0923	1.4358	23.92 %

The platform pitch motion response spectra have been computed and presented in figure 5.18. The mean pitch motion and standard deviation are computed directly from time series data, while the STD for linear dynamic model is calculated from the motion response spectra. The results are shown in table 5.10. A log-scale version of the pitch motion response spectra is given in figure 5.19.

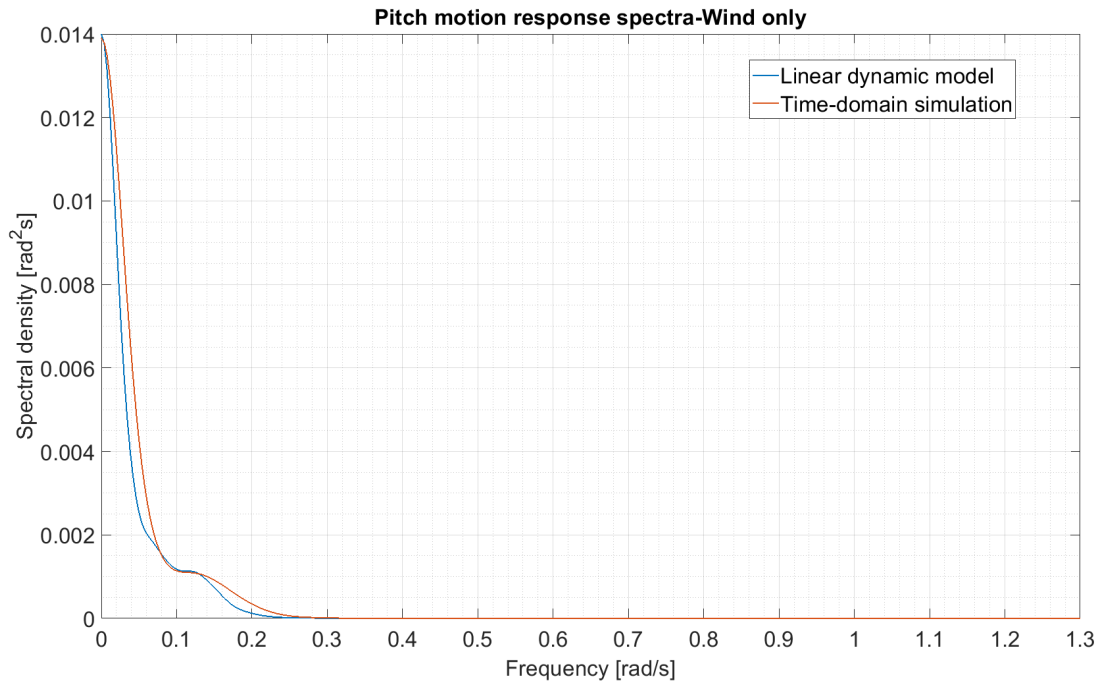


Figure 5.18: Pitch motion response spectra in wind only condition

Table 5.10: Comparison: pitch motion response spectra-wind only condition

Parameter	Linear dynamic model	Time-domain simulation	Error
Mean pitch motion	-	0.1082 rad	-
STD	0.0235	0.0261	9.96 %

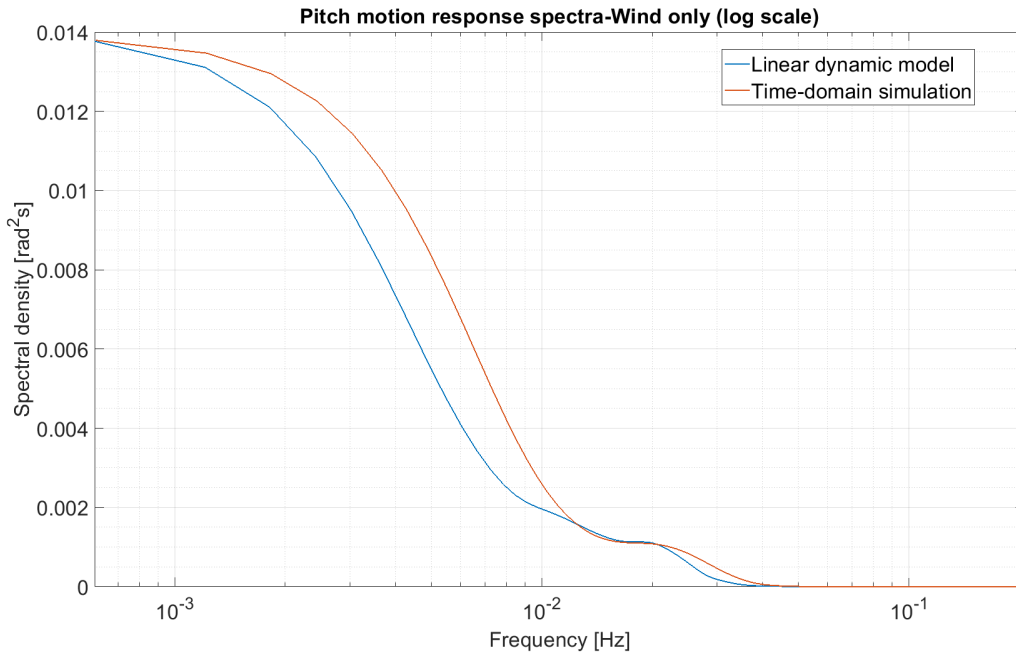


Figure 5.19: Pitch motion response spectra in wind only condition (log scale)

Still, an underestimation by linear dynamic model can be found in the low frequency range, as shown in figure 5.19.

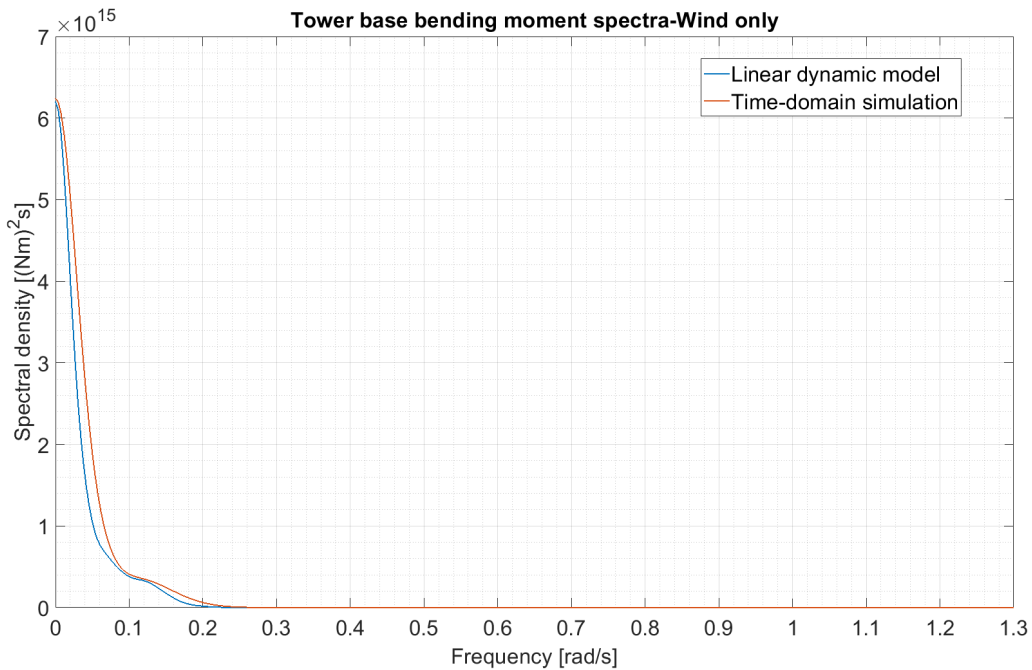


Figure 5.20: Tower base bending moment spectra in wind only condition

The spectra of tower base bending moment in wind only condition are plotted in figure 5.20. The mean value and standard deviation of the tower base bending moment have been com-

puted from time series data, in comparison with the STD calculated from response spectrum of the linear dynamic model. The results are presented in table 5.11. A log-scale version of the tower base bending moment spectra is presented in figure 5.21.

Table 5.11: Comparison: tower base bending moment spectra-wind only condition

Parameter	Linear dynamic model	Time-domain simulation	Error
Mean M_{TB}	-	7.0640e+07 Nm	-
STD	1.4949e+07	1.8556e+07	19.44 %

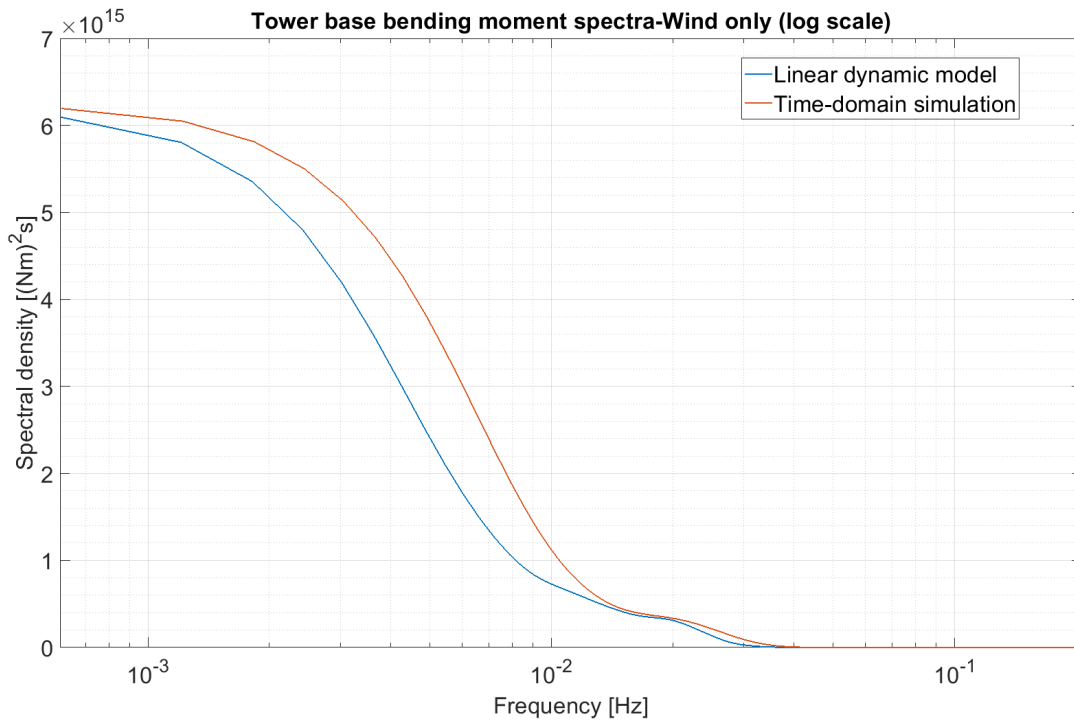


Figure 5.21: Tower base bending moment spectra in wind only condition (log scale)

It can be observed in figure 5.21 that linear dynamic model gives an underestimation in the low frequency range compared with the results from time-domain simulations. As discussed in section 5.3.1, the error may come from two parts. The underestimation of platform pitch motion will result in a decrease of bending moment contribution from wind turbine gravity loads. The rotor-average wind speed spectrum and the linearized wind turbine model may also give rise to the underestimation.

5.3.4 Discussion

After comparing the results computed by the linear dynamic model and the results obtained in fully coupled time-domain simulations for wave-only, wind-only and combined wind and wave conditions, some discussions are presented in this section.

From the results, it is clear that in wave-only condition, where the responses are mainly inertia-dominant, the developed linear dynamic model shows a good agreement with time-domain simulation results. For wind-only condition and combined wind and wave condition, the linear dynamic model gives a reasonable estimation, though an overall underestimation is noticed.

To solve the problem in frequency domain, the linearization applied might cause less accuracy in the results, which includes the calculation of aerodynamic loads based on the rotor-average wind speed spectrum. Except this, some other simplifications might also result in slight difference in the results:

- In time-domain simulations, the turbulent wind fields are fixed in the space, while the rotor disk will change its position due to platform motions and also the wind turbine deformation. The rotor-average wind speed spectrum is applied as input for the linear dynamic model. When computing the rotor-average wind speed spectrum, the centre of rotor disk is assumed to be always 90m. It might not be possible to take the rotor disk motion into account when computing the rotor-average wind speed spectrum.
- Also for the linear dynamic model, only the longitudinal component of the turbulent wind vector has been considered for simplicity, while in time-domain simulations, a 3-D turbulent wind field generated from TurbSim has been applied.
- Furthermore, in the developed linear dynamic model, the aerodynamic loads are assumed to only act on the wind turbine blades. While in the fully coupled time-domain simulations, the aerodynamic loads acting on the tower and nacelle have also been considered by using Morison model.

Chapter 6

Summary and Further Work

6.1 Summary

In this Master thesis project, a frequency-domain method in global dynamic response analysis of a semi-submersible floating wind turbine, the modified WindFloat concept design, has been studied.

A simplified linear dynamic model has been established under the selected below-rated loading condition, in which the parameters of turbulent wind and irregular waves have been defined. This linear dynamic model is developed to be used in the global dynamic response analysis. To validate the developed model, fully coupled time-domain simulations have been run in SIMA workbench for the same design and the same loading condition. Spectrum analyses have been performed for the results obtained in wave-only condition, wind-only condition and combined wind and wave condition respectively.

In general, the results presented in chapter 5 show a good agreement between the developed linear dynamic model and the time-domain simulations, which illustrates the feasibility of the developed linear dynamic model. A slight underestimation is observed when aerodynamic loads has been taken into account, which might be due to the linearization performed in order to solve the problem in frequency domain. However, the overall estimation is considered to be reasonable.

With the developed linear dynamic model, the interested system states or structural response can be investigated through transfer function or spectrum analysis. By generating re-

sponse spectra from the linear dynamic model, inverse Fourier transform can be performed to get the time series data, which can be used in fatigue analysis.

Furthermore, the method used to combine the wind turbine model and the floater together has been validated. The way to establish and linearize the constraint relationships may also be applied to combine other type of floaters and wind turbines.

6.2 Further work

In this project, the developed linear dynamic model has been validated for below-rated loading condition. Based on the results obtained, suggestions for improvement and further development are listed below:

- More structure responses can be investigated and compared, for example, the dynamic response of wind turbine blades.
- Study can be made to check the thresholds of the developed linear dynamic model, i.e. within which range, the developed linear dynamic model could give reasonable estimations.
- If corresponding linearized wind turbine models are available, linear dynamic models for another two loading conditions, above-rated condition and extreme condition, can be established and investigated.
- Second order wave loads can be taken into account in further work.
- The developed linear dynamic model can also be used in fatigue analysis and might be validated by results from time-domain methods.

Bibliography

- [1] EE. Bachynski. *Basic aerodynamics for wind turbines, Lecture material in course TMR4505 integrated dynamic analysis of wind turbines, NTNU*. 2017.
- [2] EE. Bachynski. *Lecture notes in course TMR4505 integrated dynamic analysis of wind turbines, NTNU*. 2017.
- [3] EE. Bachynski, V. Chabaud, and T. Sauder. “Real-time hybrid model testing of floating wind turbines: sensitivity to limited actuation”. In: *Energy Procedia* 80 (2015), pp. 2–12.
- [4] EE. Bachynski, M. Kvittem, and T. Luan C.and Moan. “Wind-wave misalignment effects on floating wind turbines: motions and tower load effects”. In: *Journal of Offshore Mechanics and Arctic Engineering* 136.4 (2014), p. 041902.
- [5] EE. Bachynski, T. Moan, et al. “Linear and nonlinear analysis of tension leg platform wind turbines”. In: (2012).
- [6] B. Christian et al. “The DTU 10-MW reference wind turbine”. In: *Danish Wind Power Research 2013*. 2013.
- [7] International Electrotechnical Commission et al. “IEC 61400-1: Wind turbines part 1: Design requirements”. In: *International Electrotechnical Commission* (2005).
- [8] *Column-Stabilised Units*. Standard. DNV GL, 2012.
- [9] C. Dominique R.and Christian and W. Alla. “WindFloat: a floating foundation for offshore wind turbines—part I: design basis and qualification process”. In: *ASME 2009 28th International Conference on Ocean, Offshore and Arctic Engineering*. American Society of Mechanical Engineers. 2009, pp. 845–853.
- [10] *Electric Power Monthly*. <https://www.eia.gov/electricity/monthly/>. Accessed: 2018-02-20.
- [11] EWEA. “Deep water. the next step for offshore wind energy”. In: *European Wind Energy Association report, Brussels*. See <http://www.ewea.org> (2013).

- [12] I. Fossen. *Handbook of marine craft hydrodynamics and motion control*. John Wiley & Sons, 2011.
- [13] G. Gallego and A. Yezzi. “A compact formula for the derivative of a 3-D rotation in exponential coordinates”. In: *Journal of Mathematical Imaging and Vision* 51.3 (2015), pp. 378–384.
- [14] Martin OL. Hansen. *Aerodynamics of wind turbines*. Routledge, 2015.
- [15] *Wind turbines -Part 3: Design requirements for offshore wind turbines, International Standard*. Standard. International Electrotechnical Commission, 2009.
- [16] J. Jonkman. *Definition of the Floating System for Phase IV of OC3*. Tech. rep. National Renewable Energy Laboratory (NREL), Golden, CO., 2010.
- [17] J. Jonkman. *TurbSim user’s guide: Version 1.50*. Tech. rep. National Renewable Energy Lab.(NREL), Golden, CO (United States), 2009.
- [18] J. Jonkman, J. Buhl, and L. Marshall. *Fast user’s guide-updated august 2005*. Tech. rep. National Renewable Energy Laboratory (NREL), Golden, CO., 2005.
- [19] J. Jonkman et al. *Definition of a 5-MW reference wind turbine for offshore system development*. Tech. rep. National Renewable Energy Laboratory (NREL), Golden, CO., 2009.
- [20] M. Kvittem. “Modeling and response analysis for fatigue design of a semi submersible wind turbine”. In: (2014).
- [21] M. Kvittem, EE. Bachynski, and T. Moan. “Effects of hydrodynamic modelling in fully coupled simulations of a semi-submersible wind turbine”. In: *Energy Procedia* 24 (2012), pp. 351–362.
- [22] M. Kvittem and T. Moan. “Frequency versus time domain fatigue analysis of a semisubmersible wind turbine tower”. In: *Journal of Offshore Mechanics and Arctic Engineering* 137.1 (2015), p. 011901.
- [23] M. Kvittem and T. Moan. “Time domain analysis procedures for fatigue assessment of a semi-submersible wind turbine”. In: *Marine Structures* 40 (2015), pp. 38–59.
- [24] R. Langen I.and Sigbjornsson. *Dynamic Analysis of Structures: Dynamic Analysis of Structures*. Tapir, 1979.
- [25] L. Li, Z. Gao, and T. Moan. “Joint distribution of environmental condition at five european offshore sites for design of combined wind and wave energy devices”. In: *Journal of Offshore Mechanics and Arctic Engineering* 137.3 (2015), p. 031901.

- [26] *Offshore Wind in Europe: Key trends and statistics 2017*. <https://windeurope.org/about-wind/statistics/offshore/european-offshore-wind-industry-key-trends-statistics-2017/>. Accessed: 2018-02-20.
- [27] William H. Press et al. *Numerical recipes 3rd edition: The art of scientific computing*. Cambridge university press, 2007.
- [28] *RIFLEX 4.8.4 Theory Manual*. MARINTEK, 2016.
- [29] K. Riste. “Development of a Frequency-domain Model for Dynamic Analysis of the Floating Wind Turbine Concept-WindFloat”. MA thesis. NTNU, 2016.
- [30] D. Roddier et al. “A generic 5 MW WINDFLOAT for numerical tool validation comparison against a generic spar”. In: (2011).
- [31] *SIMO 4.8.4 Theory Manual*. MARINTEK, 2016.
- [32] K. Merz. *STAS Aeroelastic 1.0-Theory Manual*. Research report. SINTEF Energi, 2018.
- [33] K. Merz. *A linear aeroelastic model of a wind turbine for integration with a floating platform*. Research report. SINTEF Energi, 2018.
- [34] K. Merz. *A linear State-Space Model of an Offshore Wind Turbine, Implemented in the STAS Wind Power Plant Analysis Program*. Research report. SINTEF Energi, 2015.
- [35] Mark W. Spong, S. Hutchinson, M. Vidyasagar, et al. *Robot modeling and control*. Vol. 3. Wiley New York, 2006.
- [36] J. Tempel. “Design of support structures for offshore wind turbines”. In: (2006).
- [37] Elizabeth N. Wayman et al. “Coupled dynamic modeling of floating wind turbine systems”. In: *Offshore technology conference*. Offshore Technology Conference. 2006.
- [38] *Wind in power 2017: Annual combined onshore and offshore wind energy statistics*. <https://windeurope.org/about-wind/statistics/european/wind-in-power-2017/>. Accessed: 2018-02-20.
- [39] *WIND POWER CAPACITY REACHES 539 GW, 52,6 GW ADDED IN 2017*. <http://www.wwindea.org/2017-statistics/>. Accessed: 2018-02-20.
- [40] *WindFloat*. <http://www.principlepowerinc.com/en/windfloat>. Accessed: 2018-02-20.
- [41] *World's first floating wind farm has started production*. <https://www.equinor.com/en/news/worlds-first-floating-wind-farm-started-production.html>. Accessed: 2018-02-20.

Appendix A

Parameter settings in TurbSim input file

Table A.1: Parameter settings in TurbSim input file

Parameter Input	Description	Value
Runtime Options		
RandSeed1	The first random seed	(Random number)
RandSeed2	The second random seed	(Random number)
WrBLFF	Write bladed-style full-field files	True
Turbine/Model specifications		
NumGrid_Z	Number of vertical grid points	32
NumGrid_Y	Number of horizontal grid points	32
TimeStep	Time step (s)	0.05
AnalysisTime	Length of analysis (s)	3900.0
UsableTime	Usable time series length (s)	3900.0
HubHt	Turbine hub height (m)	90.00
GridHeight	Height of the grid (m)	160.00
GridWidth	Width of the grid (m)	160.00
Meteorological boundary conditions		
TurbModel	Turbulence model	IECKAL
IECstandard	IEC standard	3
IECturbc	IEC turbulence	B
IEC_WindType	IEC turbulence model	NTM
WindProfileType	Type of wind profile	PL
RefHt	Reference height (m)	90.00
URef	Reference wind speed (m/s)	8.0
PLExp	Power-law exponent	0.14
Z0	Surface roughness length	0.03

The parameter settings applied in the TurbSim input file are presented in table A.1. The value is chosen based on this specific application, trade-off between simulation length and turbulent wind field mesh size, and also limitation of the computation capacity.

By giving different random numbers as inputs for parameters *RandSeed1* and *RandSeed2* while keeping the other parameters unchanged, one can generate different turbulent wind field files with certain properties of the wind fields to be the same.

Appendix B

Time vector for different variables in SIMA results

Table B.1: Time vectors for variables in SIMA results

Time vector	Parameter	Description
time_SIMO	PlatMotions	Platform positions
	PlatVelocities	Platform velocities
	wave	Wave elevation at origin
time_RIFLEX	AeroForceX	Thrust force in the shaft (local x direction)
	AeroMomX	Torque moment about the shaft
	HubWindX	Hub wind speed (local x direction)
	omega	Rotor speed
	genPwr	Generator power (including efficiency)
	TowerBaseBMY	Bending moment about local Y direction at tower base

In the SIMA workbench, the time steps for recording SIMO calculation results and RIFLEX calculation results are different input parameters. For SIMO calculation results, the setting parameter is 'Time Step' in 'Dynamic Calculation, Irreg.Analysis' section, while for RIFLEX calculation results, it is 'Displacement response storage' and 'Force response storage' in 'Dynamic Calculation, Storage' section.

In order to run the simulations with desired time steps, one must pay attention to the 'time'

vectors, especially in post-processing, since different parameters in the results may refer to different time vectors and these time vectors may not be the same.

The parameters considered in this thesis project and their corresponding time vectors are listed in table B.1. The name of the parameters refer to the 'readTimeDomainResults.mat' file, which is a MATLAB script provided by Professor Erin Bachynski at NTNU and used to read the SIMA simulation results into MATLAB. The original script has been edited to include all the interested parameters as outputs.

Appendix C

Jonswap wave spectrum

The Jonswap wave spectrum is derived in the 'Joint North Sea Wave Observation Project'. It is common to use Jonswap spectrum instead of the Pierson-Moskowitz (PM) Spectrum when one wants to express the harsh wave conditions in the North Sea. Compared with the PM spectrum, Jonswap spectrum is more narrow-banded at the peak frequency which indicates the concentration of wave energy.

As discussed in section 2.3, since the modified WindFloat concept is assumed to be located at a site in the North Sea, the Jonswap spectrum is applied. According to the RIFLEX theory manual [28], the Jonswap spectrum can be computed by:

$$S_{\xi\xi}(\omega) = \alpha g^2 \omega^{-5} \exp\left(-\beta \left(\frac{\omega_p}{\omega}\right)^4\right) \gamma^{\exp\left(-\frac{(\omega-\omega_p)^2}{2 \sigma^2 \omega_p^2}\right)} \quad (\text{C.1})$$

Where:

- ω : the wave frequency.
- ω_p : the wave peak frequency. T_p is the wave peak period.

$$\omega_p = \frac{2 \pi}{T_p}$$

- γ : Peakedness parameter.

$$\gamma = \begin{cases} 1.0; & T_p \geq 5\sqrt{H_s} \\ \exp\left(5.75 - 1.15\frac{T_p}{\sqrt{H_s}}\right) & \\ 5.0; & T_p \leq 3.6\sqrt{H_s} \end{cases}$$

- α : Phillip's constant. H_s is the significant wave height.

$$T_z = \frac{T_p}{1.407(1 - 0.287\ln\gamma)^{1/4}}$$

$$\alpha = 1.2905 \frac{H_s^2}{T_z^4}$$

- β : Form parameter. For North Sea condition, β is defined as 1.25.
- σ : Spectrum-width parameter.

$$\sigma = \begin{cases} 0.07; & \omega \leq \omega_p \\ 0.09; & \omega > \omega_p \end{cases}$$

The generated wave spectrum is presented in figure 4.5.

Appendix D

Description of the content in the attached zip-file

This appendix gives a brief description of the content in the attached zip-file which is submitted together with this Master thesis report. The zip-file includes the MATLAB scripts used to develop the linear dynamic model and some other files. The poster made for the mandatory Master thesis exhibition is also appended.

Linear dynamic model

Three file folders, **Combined Full Model**, **Waveonly Full Model** and **Windonly Full Model**, contain the MATLAB scripts created to develop the linear dynamic models under combined wind and wave condition, wave only condition and wind only condition respectively.

Read Wind Spectrum

This file folder contains a MATLAB function 'readBLgrid' in TurbSim to read the turbulent wind field files into MATLAB, and a MATLAB script to generate the rotor-average wind speed spectrum from TurbSim simulation results.

Read SIMA

This file folder contains MATLAB functions provided by Professor Erin Bachynski to read the time domain simulation results into MATLAB. It also includes MATLAB scripts to perform post-processing work, from which the operating point information can be computed and used in the linearization of constraint relationships.

TD Simulation Postprocessing

This file folder contains MATLAB functions to read the time domain simulation results into MATLAB. It also includes MATLAB scripts to get the time series data of interested parameters, which will be used as inputs to generate spectra for time-domain simulation results.

Other files in the folder

- **G1.SIF**: a WADAM analysis result file from Kristine [29].
- **Kaimal.inp**: a template of the input file to be used in TurbSim simulations.
- **readWTmartices.m**: a MATLAB script to read the linearized wind turbine model from files provided by Karl Merz.
- **sima_models.stask**: a SIMA input file provided by Professor Erin Bachynski which, which includes the SIMA model of the modified WindFloat concept.